Tectonophysics 602 (2013) 176–193

Contents lists available at SciVerse ScienceDirect

Tectonophysics

journal homepage: www.elsevier.com/locate/tecto

Interference of lithospheric folding in western Central Asia by simultaneous Indian and Arabian plate indentation

J.H.W. Smit [a], S.A.P.L. Cloetingh [b,*], E. Burov [a,c], M. Tesauro [d], D. Sokoutis [b], M. Kaban [d]

[a] ISTeP, University P & M Curie, 5, Place Jussieu, case 129, 75252 Paris Cedex 05, France
[b] Faculty of Geosciences, Utrecht University, P.O. Box 80.021, 3508TA Utrecht, The Netherlands
[c] UMR CNRS 7193, 4 place Jussieu, 75252 Paris, France
[d] GeoForschungsZentrum Potsdam, Telegrafenberg A 17, D-14473 Potsdam, Germany

ARTICLE INFO

Article history:
Received 2 March 2012
Received in revised form 9 September 2012
Accepted 30 October 2012
Available online 7 November 2012

Keywords:
Indentation
India–Eurasia collision
Arabia–Eurasia collision
Lithosphere folding

ABSTRACT

Large-scale intraplate deformation of the crust and the lithosphere in Central Asia as a result of the indentation of India has been extensively documented. In contrast, the impact of continental collision between Arabia and Eurasia on lithosphere tectonics in front of the main suture zone, has received much less attention. The resulting Neogene shortening and uplift of the external Zagros, Alborz, Kopeh Dagh and Caucasus Mountain belts in Iran and surrounding areas is characterised by a simultaneous onset of major topography growth at ca. 5 Ma. At the same time, subsidence accelerated in the adjacent Caspian, Turan and Amu Darya basins. We present evidence for interference of lithospheric folding patterns induced by the Arabian and Indian collision with Eurasia. Wavelengths and spatial patterns are inferred from satellite-derived topography and gravity models. The observed interference of the patterns of folding appears to be primarily the result of spatial orientation of the two indenters, differences in their convergence velocities and the thermo-mechanical structure of the lithosphere west and east of the Kugitang–Tunka Line.

1. Introduction

The Cenozoic collision with both India and Arabia affects Eurasia from the Aegean to the Pacific (e.g., Yin, 2010). The two indenting Indian and Arabian plates set up a stress system in the adjacent segment of the Eurasian plate northward and westward of the plate boundary, respectively (e.g., Hatzfeld and Molnar, 2010; Liu and Bird, 2008). This stress system is affecting the intraplate topography up to distances of the order of a few thousands of kilometres, leading to significant differential vertical motions.

Obviously, the India–Eurasia collision is by far the most dominating factor in the eastern segment of the Alpine–Himalayan collision belt because it has accommodated more shortening (e.g., Hatzfeld and Molnar, 2010). At the same time, the contribution of the Arabian indenter to the deformation of Central Asia cannot be neglected. The simultaneous nature of both indentations operating under a high angle generates a geometrical interference, with a plan view pattern detectable by large wavelength anomalies in gravity and surface topography (Fig. 2). The origin of this deformation has been addressed by a large body of observational and modelling studies (e.g., Agard et al., 2011; Burg and Schmalholz, 2008; van Hinsbergen et al., 2011). A number of mechanisms for the mode of intraplate deformation have been proposed, including lithosphere folding and associated brittle deformation in the upper crust (e.g., Burg et al., 1994; Burov and Molnar, 1998; Cloetingh and Burov, 2011). A striking observation is the spatial patterns in differential vertical motions in the areas west and northwest of the Tien Shan and north of the Kopeh Dagh (or Kopet Dagh), the main deformation zones related to the collision of Eurasia with the Indian and Eurasian indenters, respectively. In previous work, the effects of the combined Arabian and Indian indenters in this area have been studied on basin scale (Reiter et al., 2011), examining the thin-skinned deformation.

In this paper, we investigate whether these spatial patterns can be the result of the interference of lithospheric folding. It is common knowledge that waves with different orientations will interact with each other. Lithosphere folding, by its nature similar to a standing wave (e.g., Burov and Cloetingh, 2009; Cloetingh and Burov, 2011), is not likely to be an exception. A number of studies have investigated fold interference and fold interference patterns in geology, initially mainly from an analytical (e.g., Ramsay, 1967) and analogue modelling perspective (e.g., Ghosh and Ramberg, 1968; Ghosh et al., 1995; Grujić, 1993) and more recently through regional studies (e.g., Simón, 2004) and a numerical modelling approach (e.g., Kaus and Schmalholz, 2006; Lechmann et al., 2011; Schmalholz, 2008). In the present paper, we point out that collision of the Eurasian plate with the Arabian and Indian plates generates folding of the Eurasian lithosphere in two

* Corresponding author. Tel.: +31 30 2537314.
E-mail addresses: jeroen.smit@upmc.fr (J.H.W. Smit), sierd.cloetingh@uu.nl (S.A.P.L. Cloetingh), evgenii.burov@upmc.fr (E. Burov), magdala@gfz-potsdam.de (M. Tesauro), dimitrios.sokoutis@uu.nl (D. Sokoutis), mikhail.kaban@gfz-potsdam.de (M. Kaban).

0040-1951/$ – see front matter © 2012 Elsevier B.V. All rights reserved.
http://dx.doi.org/10.1016/j.tecto.2012.10.032

different directions with their interference manifest in the regional geology, gravity and the topography.

In the following sections, we first present an integration of observations on intraplate deformation for the areas simultaneously affected by the collision of Eurasia with Arabia and India. The observations are subsequently compared with inferences from numerical and analogue tectonic experiments. In doing so, we focus on a quantitative assessment of factors such as lateral variation in lithosphere strength, thermo-mechanical age and distance to the plate boundary on the activity of folding as a mechanism of intraplate deformation in this area.

2. Nature and timing of Neogene intraplate deformation in front of the Arabian and Indian indenters

Asia constitutes two broad Cenozoic deformation zones separated by the Afghan/Helmand block (e.g., Yin, 2010): the India–Asia collision zone in the east and the Arabia–Asia collision zone in the west (Fig. 1). To the west, the north- to northwest-trending dextral fault system on either side of the Lut block accommodates the northward indentation of Arabia into Asia. Numerous studies have addressed the strike–slip deformation in east Iran (e.g., Bonini et al., 2003; Le Dortz et al., 2011; Regard et al., 2004). Indentation of India is separated from the Afghan/Helmand block by the left-lateral Chaman Fault system (e.g., Yin, 2010) (Fig. 1). The first order spatial features of intraplate deformation are strikingly similar in the area north of the Indian and Arabian indenters (Hatzfeld and Molnar, 2010) (Fig. 2), whereas the basins and ridges in both domains show a northward younging in their inception, away from the plate boundary.

2.1. India–Eurasia collision

The collision of India with Eurasia seems to have occurred between 55 and 45 Ma, starting with thrusting in Tibet (e.g., Hatzfeld and Molnar, 2010; Yin, 2010 for review). The subsequent extrusion of SE Asia, 32–17 Ma (Yin, 2010), was one of the first far-field effects of collision on intraplate deformation to be recognised (e.g., Cunningham, 2005; Molnar and Tapponnier, 1975; Van Hinsbergen et al., 2011) (Fig. 1). The Central Asian deformation domain (Yin, 2010) is bordered by the Pamirs in the south and the Baikal rift zone in the north. The Central Tien Shan consists of an alternation of ranges and basins separated by reverse faults (Buslov et al., 2007; Cobbold et al., 1993).

Prior to ca. 25 Ma, Cenozoic intracontinental deformation was confined mostly inside Tibet. It was likely that the present Tarim and Junggar basins were linked as one unified basin at this time before the formation of the Tien Shan range, forming a broad topographic depression north of the Tibetan Plateau (Yin, 2010). A number of recent studies have provided constraints on the timing of the Neogene uplift of the Tien Shan (e.g., Charreau et al., 2009; De Grave et al., 2007; Sobel et al., 2006, 2011). Mountain growth as an effect of the India–Eurasia collision propagated northward and reached the northern Tien Shan at ca. 11 Ma and the Altai–Sayan area as well as Lake Baikal at 5 Ma (Buslov et al., 2008). To the northwest, the Kazakh Hills in Northern Kazakhstan have been subjected to denudation during the past 3 Ma. This denudation has led to extensive aeolian erosion, which suggests that the Kazakh Hills were one of the source areas of the Central Asian loess (e.g., Buslov et al., 2008).

The Tien Shan terminates west of the right-lateral Talas–Ferghana Fault by splaying into two narrow mountain chains that surround the Ferghana Valley (Figs. 2 and 3). A narrow belt of mountains parallel to the central section of the fault slopes downward to the Ferghana Valley, underlain by a deep basin with as much as 8 km of Cretaceous–Cenozoic sediments (e.g., Cobbold et al., 1993). The gravity data suggest that the Ferghana and Tadjik basins are gravitationally overcompensated, with a several kilometres deeper Moho than predicted by local isostatic models (Burov et al., 1990).

Constraints are available on present-day deformation rates from GPS and geologic slip rates along faults (e.g., Calais et al., 2006; Mohadjer et al., 2010; Reilinger and McClusky, 2011; Vergnolle et al., 2007; Zubovich et al., 2010), yielding estimates for horizontal displacement of up to 1.5 cm/yr.

2.2. Arabia–Eurasia collision

Continental collision of Arabia with Eurasia that has been active since the late Oligocene was largely accommodated along the Zagros suture zone and to a small extent along the Alborz Mountain belt during most of the Miocene (for recent reviews see e.g., Agard et al., 2011; Mouthereau et al., 2012). The formation of the East Anatolian and Iranian Plateaus as well as the Lesser Caucasus began in the Serravalian (ca. 12–14 Ma) (e.g., Dewey et al., 1986; Forte et al., 2010; Guest et al., 2006; Hüsing et al., 2009; Sengör et al., 1985). Since ca. 5 Ma, deformation moved rapidly further outward. The outward propagation is manifest in the growth of the Zagros foreland fold-and-thrust belt in the south and in the north by rapid uplift of the Alborz (Axen et al., 2001; Guest et al., 2007), Kopeh Dagh (Lyberis and Manby, 1999) and Caucasus (Avdeev and Niemi, 2011; Brunet and Cloetingh, 2003; Brunet et al., 2009; Egan et al., 2009; Forte et al., 2010; Guest et al., 2007), mountain belts that formed along old sutures separating the Iranian microblocks from Eurasia (e.g., Brunet and Cloetingh, 2003; Lyberis and Manby, 1999; Nikishin et al., 2002; Thomas et al., 1999a). These Miocene events reflect changes in the kinematic of the Arabian plateaus described from it's southern and western boundaries (e.g., Smit et al., 2010).

The Alborz Mountains, have a present-day elevation of 2–4 km and a missing crustal root (Sodoudi et al., 2009) (Fig. 4). Results from geothermochronology demonstrate a rapid phase of uplift, with rates of 0.7 km/My exhumation between 6 and 4 Ma (Axen et al., 2001), implying approximately 10 km of uplift of the Alborz Mountains. The uplift in the Alborz was nearly synchronous with rapid subsidence in the South Caspian Basin (Nadirov et al., 1997) and subsequent folding (Devlin et al., 1999). The South Caspian Basin is probably one the deepest sedimentary basins in the world with an estimated sedimentary thickness up to 20 km (e.g., Brunet et al., 2009; Mangino and Priestley, 1998). Nadirov et al. (1997) showed that South Caspian sedimentation rates locally increased more than tenfold at ca. 6 Ma, with more than 10 km sediments deposited since then. As argued by Axen et al. (2001), if approximately 10 km of post 6 Ma sediments are present in this basin, then as much as 20 km, equivalent of 80% of the structural relief of about 25 km between the high Alborz and the southernmost Caspian basement may be younger than 6 Ma. The transition between the South Caspian Basin and flanking Alborz is abrupt and coincides with a coastline bounded by a major reverse fault system. A mountain range, a few kilometres high next to a 20 km deep basin is highly anomalous in terms of differential topography. The substantial gravity anomalies have a wavelength characteristic for lithosphere scale deformation including an upper mantle component. It is exactly for this reason that various authors (e.g., Jackson et al., 2002) have emphasised the need for a contribution by lithosphere dynamics. The residual mantle gravity field, which is obtained after removing of the crustal effect from the observed data, demonstrates an exceptionally large anomaly over the basin (Kaban, 2002).

The lack of a crustal root under the Alborz Mountains points to a flexural support by the South Caspian basement. Abnormal mantle (Kadinsky-Cade et al., 1981) and late Cenozoic alkaline igneous rocks in the Alborz suggest that buoyant mantle is a factor as well (Axen et al., 2001). Guest et al. (2007) have argued in favour of compressional deformation of the South Caspian Basin/Alborz Mountains. This interpretation was largely based on available industrial seismic reflection data and gravity data for the basin and followed a similar proposition made earlier for the late stage deformation of the adjacent Black Sea (Brunet and Cloetingh, 2003; Nikishin et al., 1997; see also Munteanu et al., 2011).

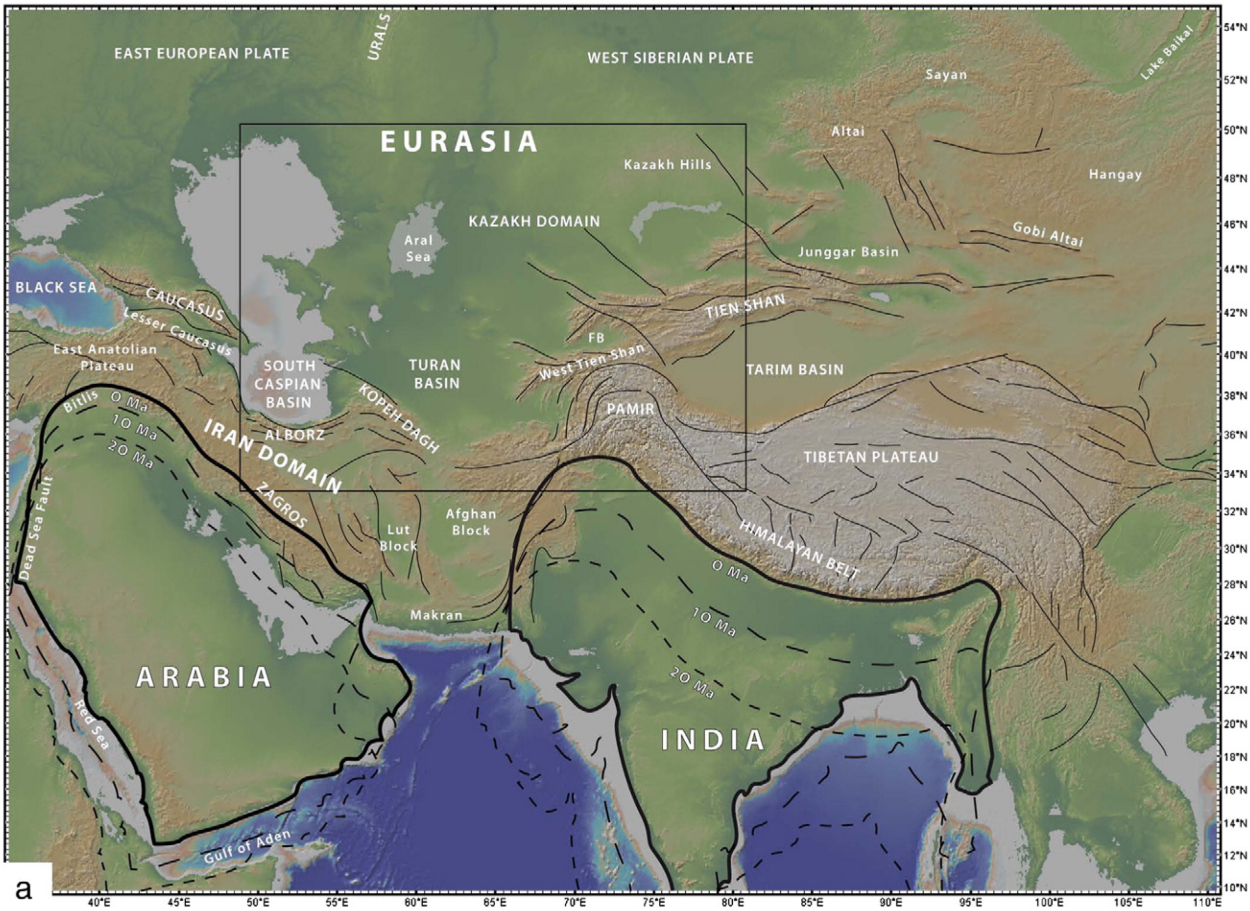
EAST EUROPEAN PLATE
URALS
WEST SIBERIAN PLATE
Sayan
Lake Baikal
EURASIA
Altai
Kazakh Hills
Hangay
KAZAKH DOMAIN
Aral Sea
Gobi Altai
Junggar Basin
BLACK SEA
CAUCASUS
Lesser Caucasus
TIEN SHAN
FB
East Anatolian Plateau
SOUTH CASPIAN BASIN
TURAN BASIN
West Tien Shan
TARIM BASIN
Bitlis
0 Ma
10 Ma
20 Ma
KOPEH DAGH
PAMIR
ALBORZ
IRAN DOMAIN
TIBETAN PLATEAU
ZAGROS
Dead Sea Fault
Lut Block
Afghan Block
HIMALAYAN BELT
Makran
ARABIA
Red Sea
INDIA
Gulf of Aden
a

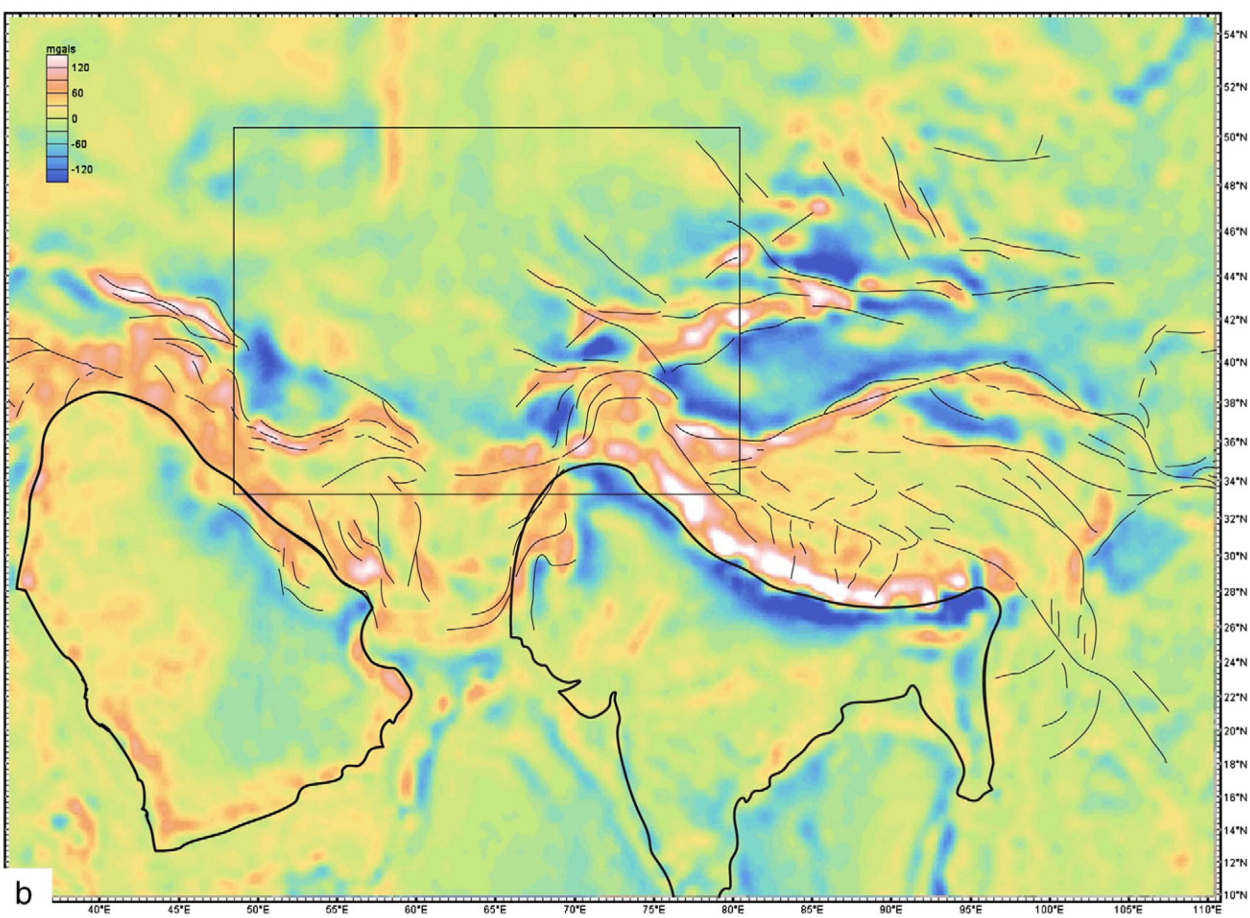
mgals
120
60
0
-60
-120
b

The Kopeh Dagh Mountains are the eastern continuation of the Alborz and formed by the inversion of an older basin along the Palaeotethys suture (Lyberis and Manby, 1999). The Amu Darya Basin north of it is part of the Turan Domain (or Turan Plate) (Figs. 2 and 3). The post-Miocene onset of inversion of the Kopeh Dagh marks the transition from asymmetrical foreland flexural subsidence to a more symmetrical subsidence in the Amu Darya Basin (Lyberis and Manby, 1999; Thomas et al., 1999a). The major depocentre axis in the centre of the basin is oriented parallel to the suture zone (Thomas et al., 1999b). Such a temporal shift appears to be a characteristic of many foredeep basins affected by late-stage compression (Cloetingh and Burov, 2011; Garcia-Castellanos and Cloetingh, 2011).

2.3. West Central Asia: the Turan and Kazakh domains

West Central Asia, the area located between the Tien Shan and the Caspian Sea and north of the Kopeh Dagh and Alborz, is characterised by a system of parallel NNW–SSE trending ridges and basins, among which the Amu Darya Basin (Figs. 2 and 3) (see also Thomas et al., 1999a). This trend is parallel to the Palaeotethys suture along the Alborz and Kopeh Dagh Mountains (Fig. 2b). These ridges and basins have a long polyphase history dating back to at least the early Mesozoic. The latest phase of renewed vertical movement has been dated as latest Neogene–early Pliocene (e.g., Thomas et al., 1999a, 1999b; Belousov et al., 2001). Evidence for active differential uplift of the mountain ridges and basins of the Turan block and the South Kazakh domain, with systematically faster uplift of the mountain ridges has been presented by Thomas et al. (1999a, 1999b) and by Jaboyedoff et al. (2005).

Reactivation and fast uplift in the Kyzyl Kum and Karatau Mountains is mainly post-Miocene (for review, see Belousov et al., 2001), contemporaneous with both the inversion of the Kopeh Dagh and the increased shortening in the Tien Shan and the Pamir (e.g., Fu et al., 2010; Heermance et al., 2008). Uplift of the series of mountain ridges is often attributed to recent dextral movement along long-lived fault zones like the Talas Ferghana Fault in the Karatau Mountains that currently moves at a rate of <2 mm/yr (e.g., Zubovich et al., 2010).

Fig. 2 displays the topography (Fig. 2a) and GRACE satellite gravity map (Fig. 2b) of Central Asia with structural trends superimposed. The young (0–10 Ma) topography of the series of parallel NW–SE trending ridges have been attributed to dextral displacement along long lived shear zones caused by the indentation of India (e.g., Zubovich et al., 2010) and to intraplate lithosphere scale deformation of the East European Platform and Central Asia (Nikishin et al., 1993, 1997).

Whereas the Kopeh Dagh, Kyzyl Kum and Karatau ranges are strikingly parallel, the geological map (Fig. 3, after Thomas et al., 1999a, 1999b) shows that the outcropping Neogene strata and its Pliocene–Quaternary sedimentary cover do not follow this pattern. Along the central axis in the northern half of the Turan Basin where the Pliocene–Quaternary units should be reaching maximum thickness, the Neogene crops out instead. The same occurs in the Syr Darya Basin. The Neogene does not outcrop along the rim of the basins as to be expected, nor does Pliocene–Quaternary thickness increase downstream the main rivers. Obviously, the outcrop pattern of the Neogene and Quaternary units as drawn in the geological map (Fig. 3b) point to a non-cylindrical deformation during Pliocene and Quaternary times. Therefore, it appears that dextral strike–slip along faults like the Talas–Ferghana Fault cannot explain the large-scale patterns of differential topography of the Turan and South Kazakh domains.

Estimates for the thermo-mechanical age, the time elapsed after the end of the last important thermal perturbation, vary from 200 to 300 Ma, corresponding to thermal resetting by the amalgamation of magmatic arcs during the Early Mesozoic Eo–Cimmerian orogeny (Garzanti and Gaetani, 2002; Thomas et al., 1999a, 1999b).

3. Thermo-mechanical structure of the lithosphere

As pointed out previously, lithospheric heterogeneity in the area is obviously playing an important role in the architecture of the deforming intraplate lithosphere. Pronounced rheological contrasts have been inferred (Tesauro et al., 2012, this volume) between the relatively weak lithosphere underlying the area of Central Asia east of the Kugitang–Tunka Line and the relatively strong lithosphere in the Turan plate, Kazakh Domain and the Caspian Basin region, both located westward of the Kugitang–Tunka Line (Fig. 5). Fig. 5a shows the depth to Moho (Kaban, 2002). Thick crust under the Caucasus and Tien Shan reflects the presence of roots separated by areas of thinner crust. Spatial variations in bulk rheology occur also in a north–south direction, with the weakest lithosphere close to the collision zone (Tesauro et al., 2012, this volume) (Fig. 5b–d). At the far north, facing the area primarily affected by the Arabian plate indenter, the strong lithosphere of the Kazakh shield forms a buttress to the deformation set up by the collision. The same is true for the West Siberian shield located at the far front of the Indian plate indenter. The contrast in thermo-tectonic age and crustal thickness leads to a relatively strong lithosphere westward of the lineament reflected in the estimate of 45–60 km for its effective elastic thickness (Fig. 5e).

4. Folding as a mechanism for intraplate deformation in front of the indenters

4.1. The concept of lithospheric folding

Lithosphere folding has been recognised as an important mode for intraplate deformation and sedimentary basin formation (e.g., Burg and Podladchikov, 1999; Cloetingh and Burov, 2011; Lechmann et al., 2011; McAdoo and Sandwell, 1985; Stephenson and Lambeck, 1985). Different simultaneously occurring wavelengths of crustal and mantle folding are a consequence of the rheological stratification of the lithosphere (Burov et al., 1993). Decoupled continental lithosphere folding has separate wavelengths for crustal and upper mantle folding (Cloetingh and Burov, 2011). Surface wavelengths can be affected also by feedback with surface processes (Cloetingh and Burov, 2011). Both analogue and numerical experiments of intraplate deformation demonstrate the direct mechanical coupling within the layered lithosphere which gives rise to large-wavelength deflection at deeper levels and short-wavelength deformation by thrusting at or near the surface (e.g., Burov and Cloetingh, 2009; Cobbold et al., 1993; Fernández-Lozano et al., 2011; Guest et al., 2007; Martinod and Davy, 1994; Schmalholz et al., 2009; Sokoutis et al., 2005). Folding leads by its nature to brittle deformation manifested in pop-up structures in the deforming lithosphere as documented by field and modelling studies (e.g., Burg and Podladchikov, 2000; Cloetingh et al., 1999; Cobbold et al., 1993; Fernández-Lozano et al., 2011; Martinod and Davy, 1994).

As pointed out by numerous quantitative studies on lithosphere folding, amplitudes and wavelengths of folding can be calculated for a given rheology and thermo-mechanical age of the lithosphere. Constraints are provided from basement deflection in the downflexed portion of the lithospheric fold and surface topography in the upward part of the fold. Both estimates are sensitive to effects of erosion and sedimentation intrinsically amplifying and reducing amplitudes

Fig. 1. a) Large overview map of Central Asia with main structural trends (modified from Hatzfeld and Molnar (2010) and Yin (2010)) and the Indian and Arabian indenters (including their convergence history with Eurasia for several time slices (modified from Hatzfeld and Molnar, 2010)). Base map is a GMRT topography image (Ryan et al., 2009). b) Gravity anomalies from GRACE satellite mission of study area with structural trends superimposed (both maps generated using GeoMapApp, http://www.geomapapp.org). B. = basin; F. = fault; R. = range.

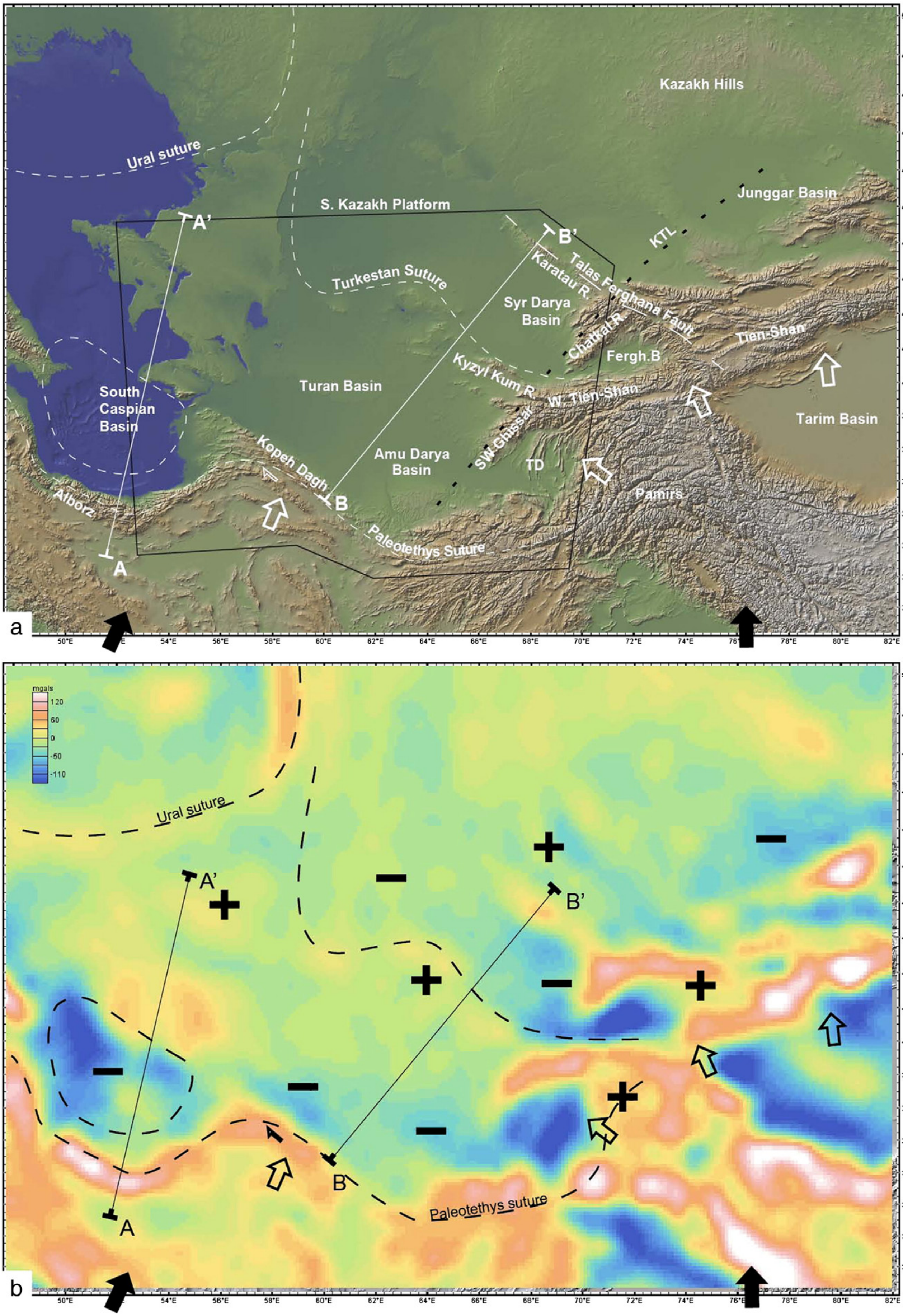
a
Kazakh Hills
Ural suture
Junggar Basin
S. Kazakh Platform
A'
B'
KTL
Turkestan Suture
Talas Ferghana Fault
Karatau R.
Syr Darya Basin
Chatkal R.
Tien-Shan
Fergh.B
South Caspian Basin
Turan Basin
Kyzyl Kum R.
W. Tien-Shan
Tarim Basin
Kopeh Dagh
SW Ghissar
Amu Darya Basin
TD
Pamirs
Alborz
B
Paleotethys Suture
A
b
mgals
120
60
0
-50
-110
Ural suture
A'
B'
Paleotethys suture
B
A
50°E
54°E
56°E
58°E
60°E
62°E
64°E
66°E
68°E
70°E
72°E
74°E
76°E
78°E
80°E
82°E
50°N
49°N
48°N
47°N
46°N
45°N
44°N
43°N
42°N
41°N
40°N
39°N
38°N
37°N
36°N
35°N
34°N
33°N

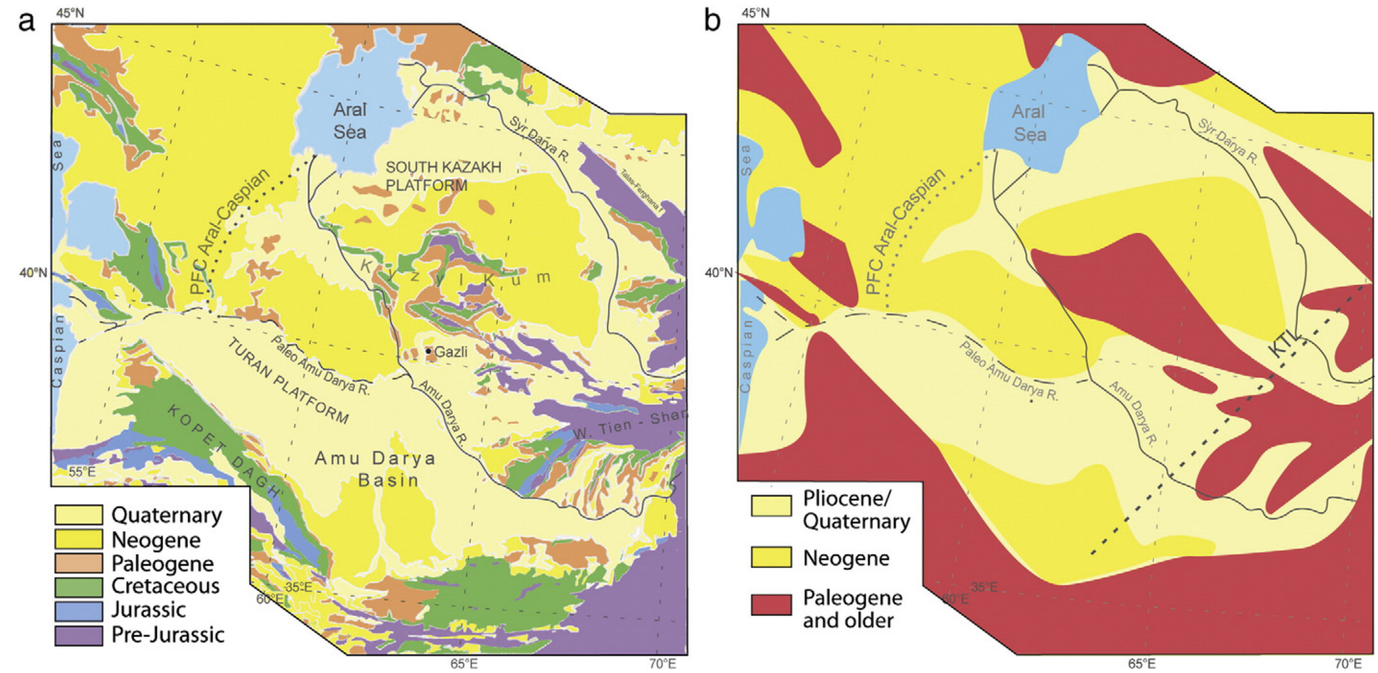

Fig. 3. a) Geological map of the Turan plate (modified from Thomas et al., 1999b) and comparison orientation of main ridges and basins and areas of differential vertical motions. Note that Neogene outcrops coincide with areas of main uplift. The area corresponds with the box in Fig. 2a. b) Simplified geological map displayed in Fig. 3a. Note that the Neogene and Pliocene–Quaternary units do not follow the expected cylindrical pattern. Instead, the Neogene crops out where the Pliocene–Quaternary units should be thickest. Solid and dashed lines mark locations of current and palaeo fluvial connections (PFC).

respectively. In addition, constraints on amplitudes are provided by gravity and seismic data and Moho deflection. It is now recognised and supported by both numerical (e.g., Burg and Podladchikov, 2000; Cloetingh et al., 1999; Guest et al., 2007; Lechmann et al., 2011; Schmalholz et al., 2009) and analogue modelling studies (e.g., Burg et al., 1994; Cobbold et al., 1993; Davy and Cobbold, 1991; Sokoutis et al., 2005) that folding of the lithosphere, involving its synclinal as well as anticlinal deflection (Figs. 6 and 7), in general plays a more important role in the large-scale deformation of intraplate domains than hitherto realised (Burg and Podladchikov, 2000; Cloetingh et al., 1999; Guest et al., 2007; Holford et al., 2009; Shin et al., 2009). These studies showed that folding starts to develop from the beginning of compression and does not always require large intraplate stresses (Bourgeois et al., 2007; Burov et al., 1993; Cloetingh et al., 1999; Fernández-Lozano et al., 2011; Gerbault et al., 1999; Nikishin et al., 1993, 1997).

Folding as a mode for intraplate deformation is closely related to transmission of intraplate stress fields away from plate boundaries into continental interiors (Van der Pluijm et al., 1997; Ziegler et al., 1998), affecting rifted continental margins (Johnson et al., 2008; Muñoz-Martín et al., 2010) and back-arc basins (Dombrádi et al., 2010) as well. Folding has important implications for vertical motions, sedimentary basin architecture and the evolution of hydrocarbon systems (e.g., Cloetingh et al., 2010; Ziegler et al., 1995, 1998).

4.2. Characteristics of lithosphere folding in front of the Indian indenter

Early studies of the effects of India–Eurasia collision on intraplate deformation have demonstrated the existence of large-scale folding in the oceanic lithosphere in the Bay of Bengal (Geller et al., 1983; Gerbault et al., 1999; McAdoo and Sandwell, 1985; Stein et al., 1989). Subsequent studies have drawn attention to the folding of continental lithosphere in Central Asia northward of the Indian indenter, expressed both in topography and gravity (Fig. 1) (e.g., Burg et al., 1994; Burov and Molnar, 1998; Cobbold et al., 1993; Nikishin et al., 1993, 1997). The inferred wavelength of these active tectonic lithosphere folds from prominent examples such as the Ferghana, Tadjik and Tarim basins, is consistent with the general relationship, established on the base of a global inventory of lithospheric folds (Cloetingh and Burov, 2011), between the wavelength of lithospheric folds (typically in the order of several hundreds of kilometres) and the thermo-tectonic age of the lithosphere (Fig. 6a, b). At the same time, smaller crustal folds have been detected in these areas.

The young Ferghana, Tadjik and probably Junggar basins, located northwest and north of Pamir and south of the Tien Shan ranges, underwent Jurassic rejuvenation and are therefore characterised by relatively young thermo-mechanical ages (150–175 Ma, the time elapsed after the end of the last important thermal perturbation) (Burg et al., 1994; Burov and Molnar, 1998). These basins probably have a weak lower crustal rheology (quartz-dominated), resulting, together with the relatively young thermal age in low observed values for the effective elastic plate thickness of the order of 15 km (Burov et al., 1990, 1998; Kogan and McNutt, 1987).

The approximately north–south shortening of the relatively thin lithosphere, at a present-day shortening rate in the order of 10 mm/yr, has created mountains north and south of these basins, has warped the basement of the immediate surroundings of each basin up by folding the mantle lithosphere, and has forced the basin floor down. For the Ferghana Valley, the estimated folding wavelength is in the order of 200–250 km, possibly associated with localised mantle deformation (e.g., Burov et al., 1998; Cobbold et al., 1993). It appears that the pre-existing thermal structure and variations in crustal thickness have played a major control on the styles and distribution of the intraplate deformation in this region (Fig. 2) (e.g., Burov et al., 1998).

Fig. 2. a) Topography, also shown are the locations of main suture zones. Open and closed arrows mark the orientation of main regional compression (Liu and Bird, 2008; Mohadjer et al., 2010) and the direction of plate convergence, respectively. Fergh. B., Ferghana Basin; KTL, Kugitang–Tunka Line; TD, Tadjik Depression, (for location see Fig. 1). The inset corresponds with Fig. 3. b) GRACE gravity anomaly map of western Central Asia and comparison with main directions of regional compression, plate convergence and orientation of main ridges and basins. Also shown are main areas of uplift (+) and subsidence (−). Figure conventions as in Fig. 2a.

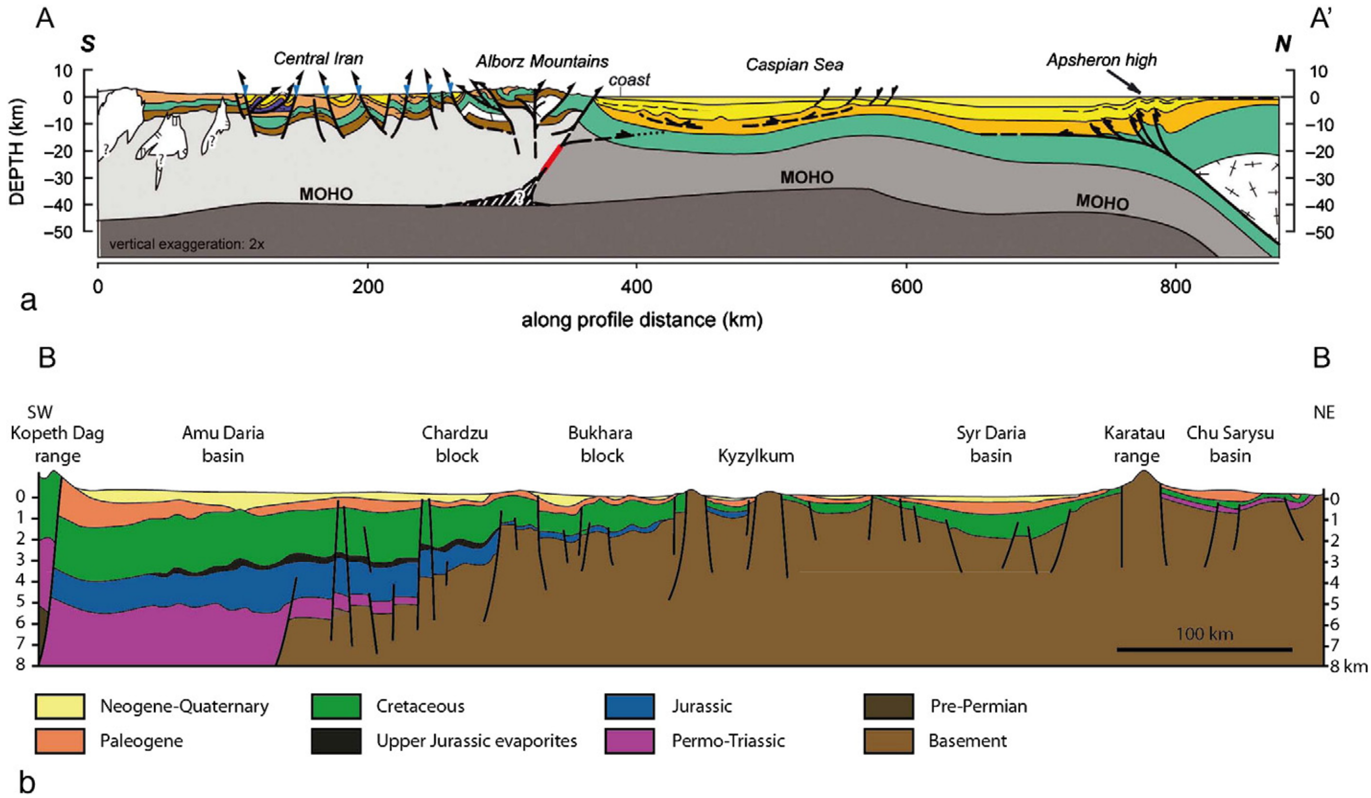

Fig. 4. Cross sections through the lithosphere of Alborz Mountains and the Caspian Basin and through the Turan and South Kazakh domains, (see Fig. 2a, b for location). a) Schematic north–south trending cross section A–A′ illustrating the basic tectonic setting for northern Iran and the South Caspian Basin (Guest et al., 2007). b) Line B–B′ indicates cross-section through the Turan and South Kazakh domains drawn by VNIGNI from seismic data (bottom) (Thomas et al., 1999b).

Primary faults, with spacing proportional to brittle layer thickness, probably appeared before folding developed, but since then the two processes, faulting and folding, co-exist in such a way that faulting is accommodated by folding with faults localised at the inflection points of folds (e.g., Cloetingh et al., 1999; Gerbault et al., 1999; Martinod and Davy, 1994). At this stage, the appearance of faults does not significantly influence the wavelength of folding. Because of the weakness of the lower crust, the upper crust is completely decoupled from the mantle and interacts with it only by flow in the lower crust.

In the area of the Tarim Basin, with a thermo-mechanical age of 400 Ma, mantle and crustal wavelengths are 360 and 50 km, respectively. At the northern margin of the Tarim Basin, sediments are deposited over a more than 350 km wide area. These wavelengths suggest a dominant control by mantle or whole lithospheric folding. In contrast, the geometries imaged by the 1000 km long deep seismic refraction profile in the northern margin of the Tibetan Plateau reveals the existence of basins with typical widths of 50–100 km (Liu et al., 2006), suggesting a control by crustal scale folding. It should be noted that results of deep refraction/wide angle reflection profiling for the southeastern margin of the Tibetan Plateau (W. Mooney, pers. comm., 2008) provides evidence for folded lithosphere overlain by sedimentary basins with typical widths of 200–250 km. The associated mechanical coupling between deforming crust and mantle lithosphere is consistent with detected folding wavelengths of the order of 350–450 km, and predictions from numerical modelling (Fig. 6b) (Cloetingh and Burov, 2011).

The present-day regional velocity and stress field in Central Asia (e.g., Liu and Bird, 2008) show an outward movement perpendicular to the NE–SW-oriented Kugitang–Tunka Line (KTL). Therefore, this would be a logical orientation for young lithosphere folding, if there is any. The southwest Ghissar and the Chatkal ranges have an odd orientation compared to the nearby ranges but are parallel to the KTL. Although obscured by the NW–SE oriented mountain ridges, a pattern of KTL-parallel uplift and subsidence does emerge from topography, gravity and especially surface geology (Fig. 8b).

4.3. Characteristics of lithosphere folding in front of the Arabian indenter

Wavelengths for compressional folding of the lithosphere in northern Iran and the South Caspian Basin are typically in the range of 400 km (Fig. 4). Although the actual basin mechanism for the formation of the Caspian Basin is not well resolved, late Neogene folding has been affecting a lithosphere probably thermally reset by middle late Jurassic marginal basin formation (Guest et al., 2007) with a thermo-mechanical age at the onset of collision of 130–150 Ma.

The deepest synclinal basins such as the South Caspian Basin can be found close to the plate contact where stresses reach maximum levels. Both numerical and analogue models predict preferential development of deep and wide synclinal basins flanked by more modest and relatively narrow anticlinal topographic heights (e.g., Fig. 7b). Sedimentation in the synclinal basins and erosion from uplifted highs further amplifies the differential topographic signature of folding.

Like the Alborz, the Kopeh Dagh and the South Caspian Basin, the area located between the Tien Shan, the Caspian Sea and north of the Kopeh Dagh, is undergoing renewed differential vertical movements since the latest Neogene–early Pliocene (e.g., Belousov et al., 2001; Jaboyedoff et al., 2005; Nikishin et al., 1997; Thomas et al., 1999a, 1999b). Reactivation and fast uplift in the Kyzyl Kum and Karatau Mountains are contemporaneous with both the inversion of the Kopeh Dagh and the increased shortening in the Tien Shan and the Pamir (e.g., Fu et al., 2010; Heermance et al., 2008). Contemporaneous differential vertical motions of a series of parallel mountain ranges and sedimentary basins over such a large area are a strong indicator for

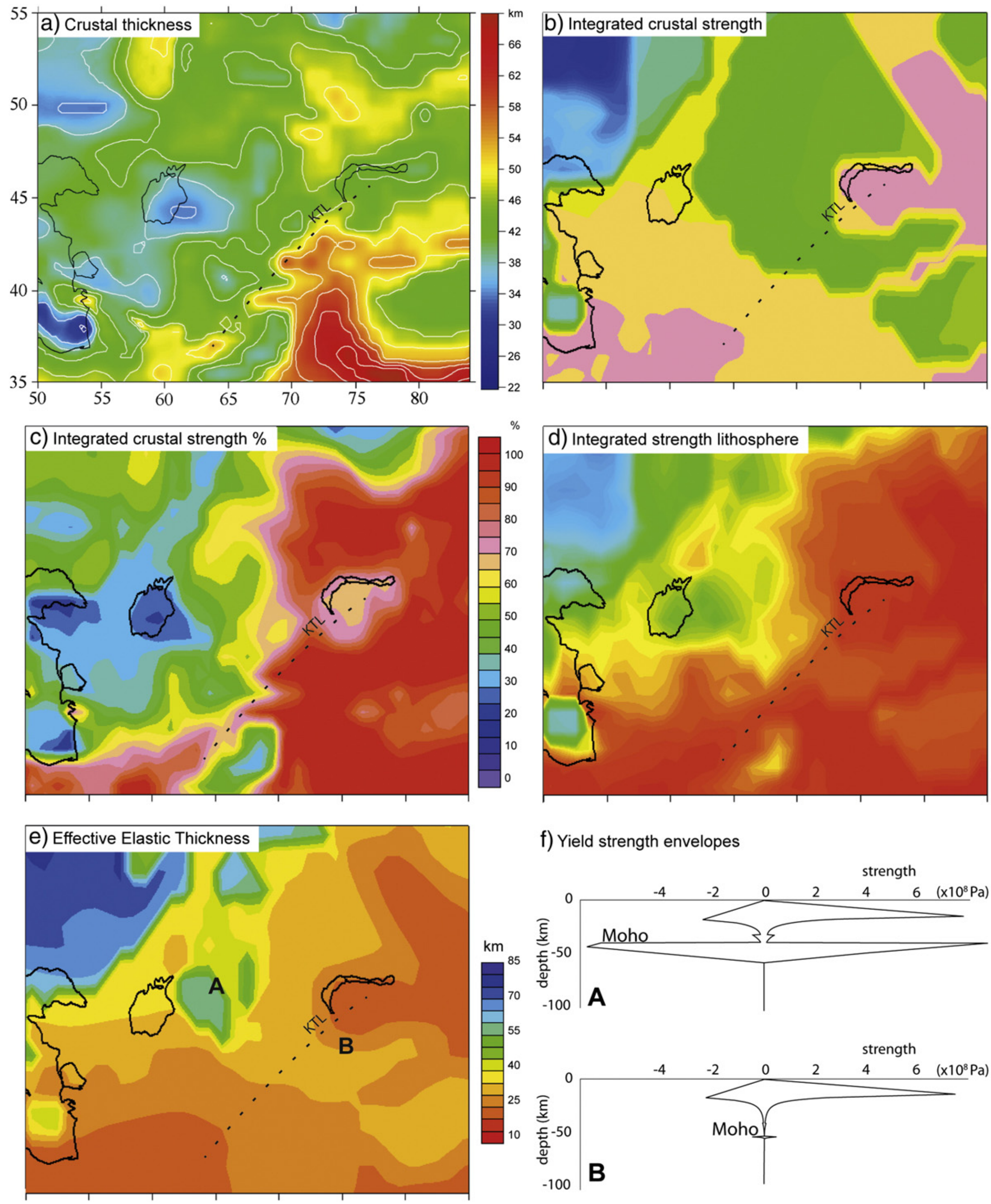

Fig. 5. Models for structure and strength for crust and lithosphere. a) Depth to Moho map (km) from Kaban (2002). Thick crust under the Caucasus and Tien Shan reflects presence of roots. b) Integrated strength (Pa m) in compression for the crust. c) Contribution of the crust to total strength (in percentage). d) Total integrated strength for crust and mantle. e) Effective elastic thickness (Te) of the lithosphere (km) estimated from the strength envelopes displayed in Fig. 5f (see Tesauro et al., 2013–this issue, for further explanations). Capital letters depict the location for which the strength profiles have been calculated. f) Yield strength envelopes in point A (top) located in the area westward and point B (bottom) located in the area eastward of the Kugitang–Tunka Line, respectively. For convention, values estimated under compressional and extensional conditions are given as positive and negative, respectively.

lithosphere folding. A thick crust and a weak rheology, characterised by estimates for the effective elastic thickness of the order of 25–30 km (Fig. 5e) are present in western Central Asia. This lithospheric configuration promotes mechanical decoupling of the crust and upper mantle lithosphere, as indicated in the strength distribution (Fig. 5f, profile A). This feature appears to be consistent with the observation of different wavelengths for crust and mantle folding of 50–70 km and 300–400 km, respectively (Fig. 8c).

4.4. Folding interference in western Central Asia

In the previous two sections, we have described indications for two, almost perpendicular, directions of lithosphere scale folding in western Central Asia (Fig. 8). The one related to the Indian indenter is NE–SW oriented and perpendicular to the Kugitang–Tunka Line, the other one is related to the Arabian indenter folds and parallel to the NW–SE oriented Kopeh Dagh. Clearly, the latter is more

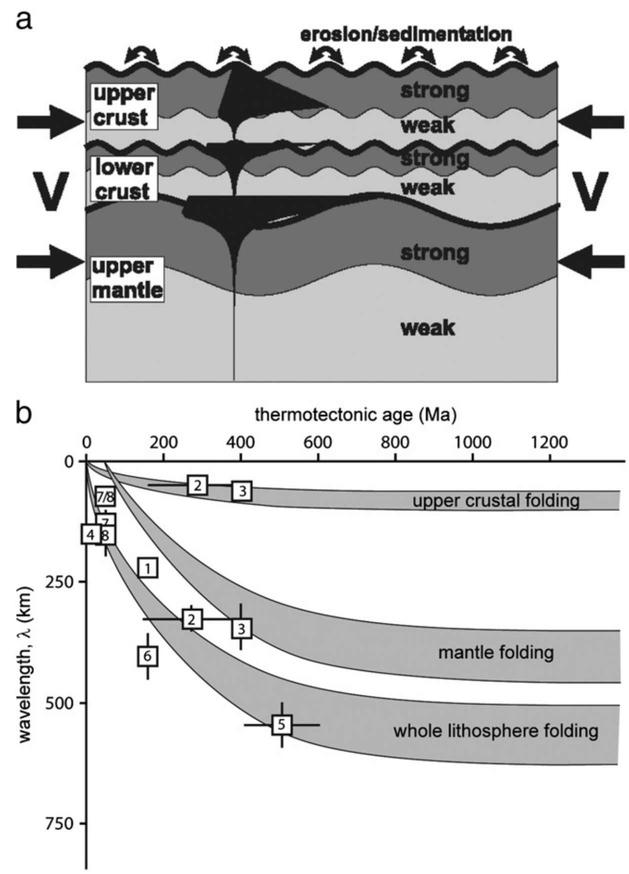

Fig. 6. Concept of folding in rheologically stratified lithosphere and feedback with sedimentation in down-folded areas and erosion of adjacent highs. b) Relationship between wavelengths of lithospheric folding and thermo-tectonic age of lithosphere. The grey zones correspond to theoretical folding wavelengths derived for the upper crust, mantle and coupled crust–mantle, based on an analytical model that accounts for strength variations as a function of thermo-mechanical age (Cloetingh et al., 1999). Squares are estimates for wavelengths of differential topography and thermo-tectonic ages inferred from observational studies in the area of investigation. Numbers refer to sites listed in Table 1.

pronounced but the KTL-parallel folds are recognisable as well. Combined, the two sets of India- and Arabia-related lithosphere folds generate an "egg-box" pattern with accentuated positive and negative differential topography that may help to explain the outcrop pattern of Neogene units (Fig. 8b).

5. Numerical and analogue modelling experiments

Numerical modelling and analogue modelling provide a framework to examine the fine structure of the interference and the localisation of deformation. Both complementary approaches provide evidence for partial mechanical coupling of the lithosphere in the folded regions. In particular, the analogue models provide a plan view perspective that demonstrates the propagation of intraplate deformation away from the plate contact. On the other hand, numerical models (e.g., Burov and Cloetingh, 2009; Kaus and Schmalholz, 2006; Lechmann et al., 2011, see also Supplementary material in Appendix A) allow us to take into account thermally dependent rheology of the lithosphere as well as to test the impact of small scale lateral variations in the rheological properties. A number of studies have numerically modelled 3D folding and studied fold interference and fold amplification for different horizontal shortening scenarios (e.g., Kaus and Schmalholz, 2006; Schmid et al., 2008). Lechmann et al. (2011) have investigated 3D folding as a result of indentation for the India–Asia collision using a full 3D numerical model.

5.1. Numerical experiments

As demonstrated by numerical models (Figs. 9 and 10), compressional basins that develop as a result of periodic folding are highly symmetrical, with dimensions that can vary from 50 to 600 km, such as observed in Central Asia (Burov and Molnar, 1998), depending on lithospheric age and shortening rate. These basins can accumulate thick sedimentary sequences up to the order of 20 km, compatible with observations from the South Caspian Basin discussed previously (Fig. 4a). The time scales associated with this process of basin formation are very short, typically a few million years (see also Cloetingh and Burov (2011) for review). The subsidence is so fast that erosion and sediment supply at the basin formation stage typically lag behind, leading to the development of starved basins, followed by shallowing upward sequences after stress relaxation. Subsidence patterns are characteristically convex upwards with time. A noticeable feature is the development of significant topography of the order of several kilometres flanking the synclinal depression. No initial heating is predicted, with an increase in heat flow with time following the basin formation. Significant brittle deformation is expected to occur in the folded basement, accelerating during the folding phase.

Figs. 9 and 10 show the results of the numerical experiments for two different thermo-tectonic ages of the lithosphere, compressed at rates of 1.25 cm a^{-1}. These strain rates are consistent with GPS data from the Tien Shan and geological slip-rates along faults (e.g., Calais et al., 2006; Vergnolle et al., 2007).

As shown, folding is well developed for both medium (250 Ma) (Fig. 9) and older (500 Ma) (Fig. 10) ages of the lithosphere. The deformation is characterised by long mantle wavelengths (360 km) and high surface amplitudes (2000 m after 10 Ma). These experiments (specifically for 250 Ma) compare well with observations from Western Goby and the Ferghana Basin in western Central Asia (Burov and Molnar, 1998; Burov et al., 1993). At late stages (10–26 Ma since the onset of shortening for 3 cm/yr or 20–50% of shortening), folding becomes aperiodic, sometimes leading to mega-folding (Burg and Podladchikov, 1999, 2000; Cloetingh et al., 1999) and the subsequent formation of high-amplitude crustal down-warps. The amplitude of vertical movements may reach 20 km or even more. As pointed out earlier, such high amplitudes of vertical motions are observed in the South Caspian Basin (Fig. 4a) (Guest et al., 2007). However, it may be relatively rare for folding to continue for periods in excess of 10 Myr. More typically is that at a certain stage deformation localises along single major fault zones (Cloetingh et al., 1999; Gerbault et al., 1999). The transition from lithospheric folding to localised shearing has also been quantified and explained as a result of viscous shear heating in Burg and Schmalholz (2008) and Schmalholz et al. (2009). As was discussed by Bird (1991), Avouac and Burov (1996) and Cloetingh et al. (1999), large-scale undulations of the lithosphere cannot be preserved for a long time (longer than 10 Myr) in the absence of sufficient compression, except for plates with very strong (especially lower crustal) rheology. Otherwise, the folds either will be flattened by gravity-driven crustal flow associated with the large crust–mantle density contrast at the Moho, or deformation will localise along some of the faults created at the inflection points of folds. It is noteworthy that interactions between short crustal and longer mantle wavelengths of folding are most pronounced at some intermediate stages of convergence, where the total amount of shortening is on the order of 20–30%. At larger amounts of shortening, short-wavelength deformation is less well expressed compared to the long-wavelength deformation, basically due to partial coupling of folded layers at large-scale fold limbs. At small amounts of shortening (ca. 10%), short-wavelength deformation is more pronounced than long-wavelength deformation. In most cases (lithosphere ages from 250 to 500 Ma) slow convergence (<1.5 cm a^{-1}) generally leads to notable development of short-wavelength crustal folding while long-wavelength mantle folding has no time to overprint short-wavelength deformation within a 20–30 Myr time window. The most prominent

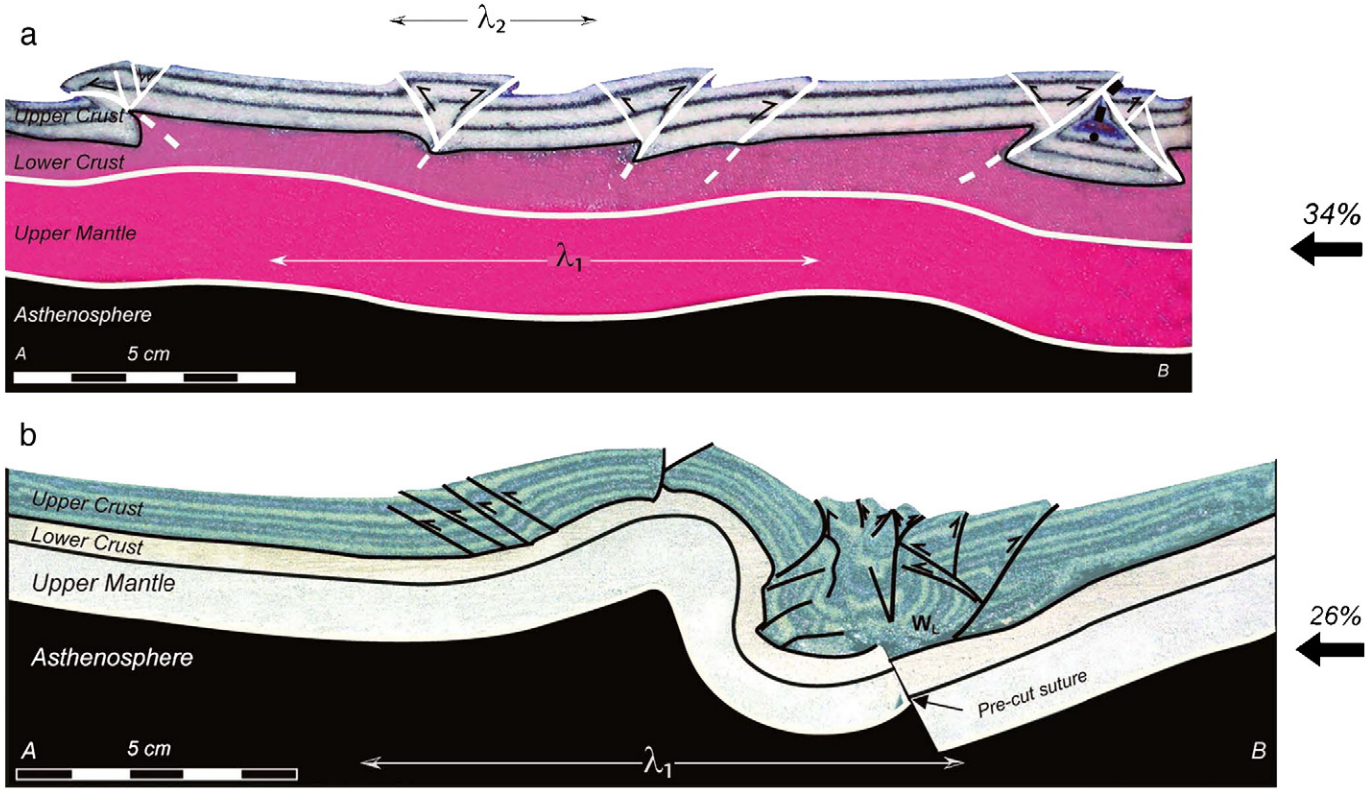

Fig. 7. Results of analogue tectonic experiments for lithospheric folding (after Sokoutis et al., 2005). Top (a) uniform lithosphere with a strong mantle. Cross section shows pop-up structures in the upper crust above highs consistent with lithospheric folding. The strong mantle allowed amplified folding of the experimental lithosphere, λ_1 and λ_2 indicate 1st and 2nd-order wavelengths, respectively. Note the similarity to Central Asia and the Amu Darya Basin (Fig. 4b). Bottom (b) Non-uniform lithosphere with suture zone, overlain by a 'mega' syncline. Note the similarity with the South Caspian Basin (Fig. 4a).

interactions between the short-wavelength and long-wavelength folding are observed for shortening rates of 3 to 5 cm a^{-1}. In this case all wavelengths develop by 10 Ma and start to interact with each other. These interactions may have different effects. In some cases short wavelength deformation is simple superimposed on long-wavelength deformation. In other cases, when the wavelengths of the crustal and mantle folding differ from each other by a factor smaller than 2–3, the results of inter-layer interactions may be highly counter-intuitive. For example, "phase shifts" in deformation of upper and lower layers may result in regional reduction or amplification of amplitude of folding and in the formation of completely a-periodic structures.

Fig. 11 shows the temporal evolution of topography in 2D and 3D view for slow and fast shortening of thermo-mechanical numerical models of a stratified 250 and 500 Ma old continental lithosphere. This figure illustrates the temporal development of short crustal wavelengths superimposed on large-scale mantle wavelengths. As shown by the numerical experiments, distributed brittle faulting occurs in the upper crust with a spacing controlled by the folding wavelength. Enhanced distributed brittle faulting may occur at different spatial scales determined by the internal structure of the lithosphere (Cloetingh and Burov, 2011).

5.2. Laboratory experiments

The laboratory experiments presented later in this paper allow tracking the 3D nature of oblique indentation by the two Indian and Arabian plates controlling the intraplate deformation in western Central Asia. In the weakened lithosphere in front of the Indian indenter, folding is trending parallel to the plate contact. Northwest of the obliquely trending Kugitang–Tunka Line, fold axes in the relatively stronger western Central Asian lithosphere further away from the plate contact rotate to an orientation parallel to this line. Analogue models show that the presence of heterogeneities such as contrasts in lithospheric properties across a suture zone exerts a main control on the mode of lithospheric folding. Folding of a uniform lithosphere is characterised by an alignment of thrust belts at the peripheral boundaries at the areas experiencing regular folding with similar amplitudes for elevated areas and folded down depressions. Brittle deformation dominated by the formation of pop-up structures in the upper crust is

Table 1
Wavelengths and ages of folded lithosphere displayed in Fig. 6 (see Fig. 1 for location). Th-tect age = thermo-tectonic age; cr = crust; l-m = lithospheric mantle.

No.	Area	Th.-tect. age (Ma)	Wavelength, (km)	References
1	Tien Shan	175	200–250	Burov and Molnar (1998); Burg et al. (1994)
2	Western Goby	175–400	300–360	Nikishin et al. (1993); Burov et al. (1993)
3	Central Asia	370–430	50–70 (cr); 300–400 (l-m)	Nikishin et al. (1993); Burov et al. (1993)
4	Himalayan syntaxis belt	8–10	150	Burg and Podladchikov (1999)
5	Russian platform	400–600	500–600	Nikishin et al. (1997)
6	South Caspian Basin	125–155	350–450	Guest et al. (2007)
7	Eastern Black Sea	40–80	50–100 (cr); 100–150 (l-m)	Cloetingh et al. (2008)
8	Western Black Sea	75	50–100 (cr);100–200 (l-m)	Cloetingh et al. (2008)

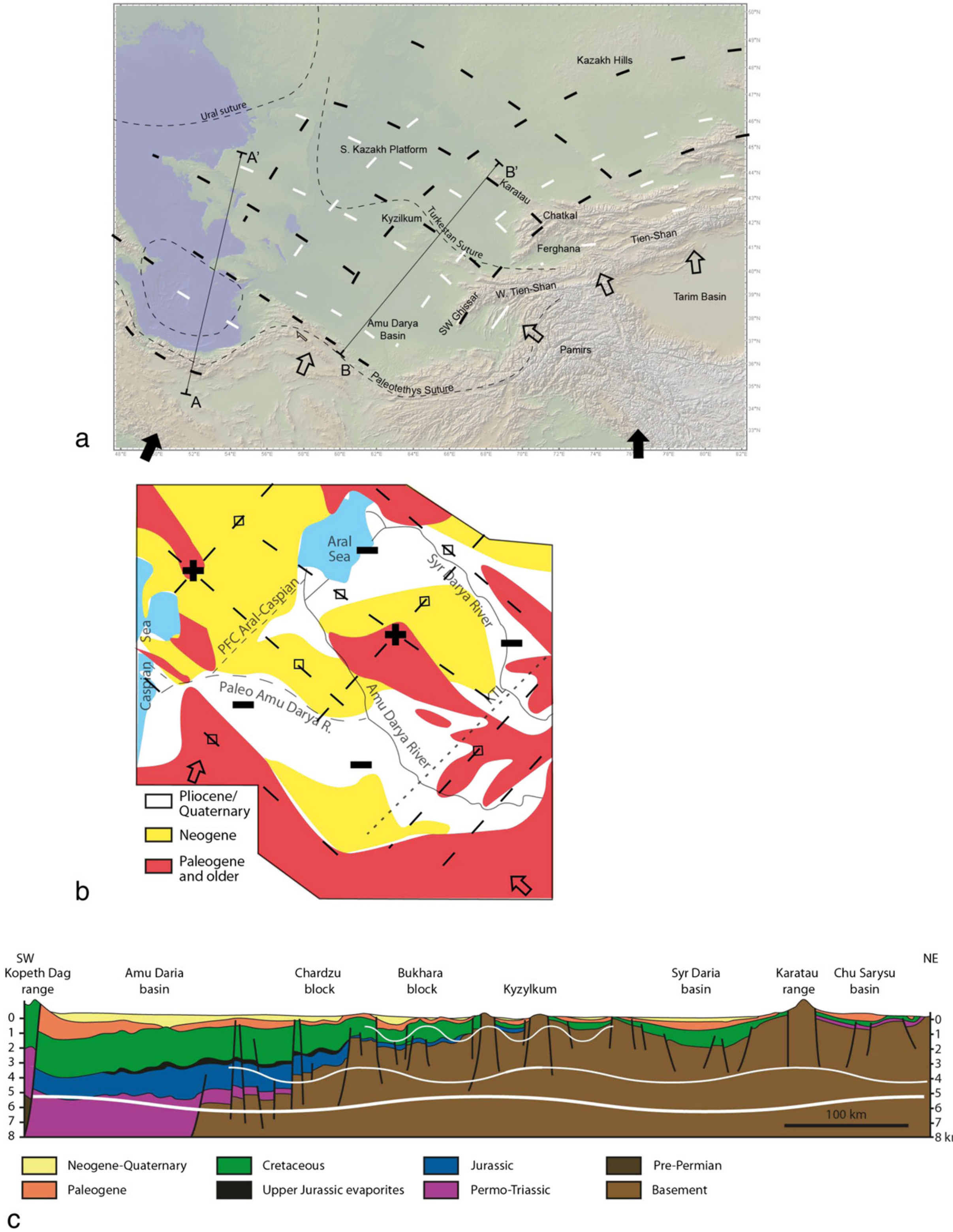

Fig. 8. a) Topography, also shown are the locations of main suture zones. Black and white dashed lines mark main fold axes. Open and closed arrows mark the orientation of main regional compression (Liu and Bird, 2008; Mohadjer et al., 2010) and the direction of plate convergence, respectively. The area corresponds with the box in Fig. 1. Also shown are main areas of uplift (+) and subsidence (−). Figure conventions are as in Fig. 2a. b) Simplified geological map of the Turan Platform (modified from Thomas et al., 1999b) and comparison with main fold axes and areas of differential vertical motions. Note that Neogene outcrops coincide with areas of main uplift. The area corresponds with the box in Fig. 2a. c) Section B–B′ through the South Kazakh and Turan domains (Fig. 4b) including folding patterns corresponding to wavelengths of 50 (top), 100–275 (middle) and 400 km (bottom), respectively.

an intrinsic feature of this mode of folding (Fig. 7a). In contrast, the presence of a suture zone promotes syncline development leading to ultra deep sedimentary basins with a depth of depression far in excess of the amplitude of the adjacent anticline. This mode of folding is characterised by a pattern of thrusting and upper crustal deformation markedly different from the model displayed in Fig. 7a.

Analogue experiments allow inspection of the three dimensional nature of lithospheric deformation. Of primary control appears to be the contrast of strong and weak lithosphere and its orientation (for a general discussion, see Sokoutis et al., 2005). Fig. 12 presents a surface view of an experiment of oblique indentation, showing stress transfer across the plate boundary that generates plate boundary parallel folding. Collision with a strong indenter block induces two sets of perpendicularly trending axes of lithospheric folding in the surrounding foreland domain. The free boundary at the right hand side, a common way to allow for lateral escape, diminishes the impact of folding in the upper right part of the deformed area. As shown by the experiment, stresses can propagate over distances several orders larger than the system's thickness. The wavelength of deformation does not appear to vary with distance from the plate boundary, whereas amplitudes show a gradual decay away from the plate boundary contact. The strong lithosphere is much less deformed than the foreland lithosphere but is affected by folding as well as faulting (Fig. 12). A striking result is that a rather uniformly distributed, low amplitude-large wavelength folding is already initiated shortly after the onset of collision (Fig. 12). With time, amplitudes rise with localisation of folding.

6. Discussion

A careful analysis of geological data, satellite-derived topography and gravity models demonstrates the existence of spatial patterns of intraplate deformation in western Central Asia. The synchronous subsidence and uplift of parallel basins and ridges that are located at relatively large distances from the main collision zones requires a lithosphere scale explanation. As illustrated in this paper, the outcrops of Neogene strata and its Pliocene–Quaternary sedimentary cover form an irregular, non-cylindrical pattern. The Neogene does not outcrop along the rim of the basins as to be expected, nor does the thickness of Pliocene–Quaternary units increase downstream the main rivers. Obviously, the outcrop pattern of the Neogene and Quaternary units as drawn in the geological map (Fig. 3b) points to a non-cylindrical deformation during the Pliocene and Quaternary. Dextral strike–slip along faults like the Talas–Ferghana Fault, or cylindrical lithosphere scale folding can explain the large-scale patterns of differential topography of the Turan and South Kazakh domains. Lithosphere folding of the Eurasian lithosphere in front of both India and Arabia has been postulated before. Taking into account that Arabia and India both excert pressure on the Turan plate and South Kazakh domain at high angles of each other (see Fig. 2 for motion vectors), non-cylindrical deformation is to be expected. Later, we discuss inferences from our analysis on the intraplate deformation of western Central Asia obtained from a comparison of observations and outcomes of analogue modelling and numerical modelling presented in this paper. In doing so, we focus on testable expressions in terms of geological and geophysical observables, allowing to discriminate lithospheric folding as a mode of intraplate deformation from other mechanisms. These observables include wavelengths and spatial patterns of intraplate deformation. We also discuss the temporal aspects of the connection between continental collision and intraplate deformation. In addition, we examine the link

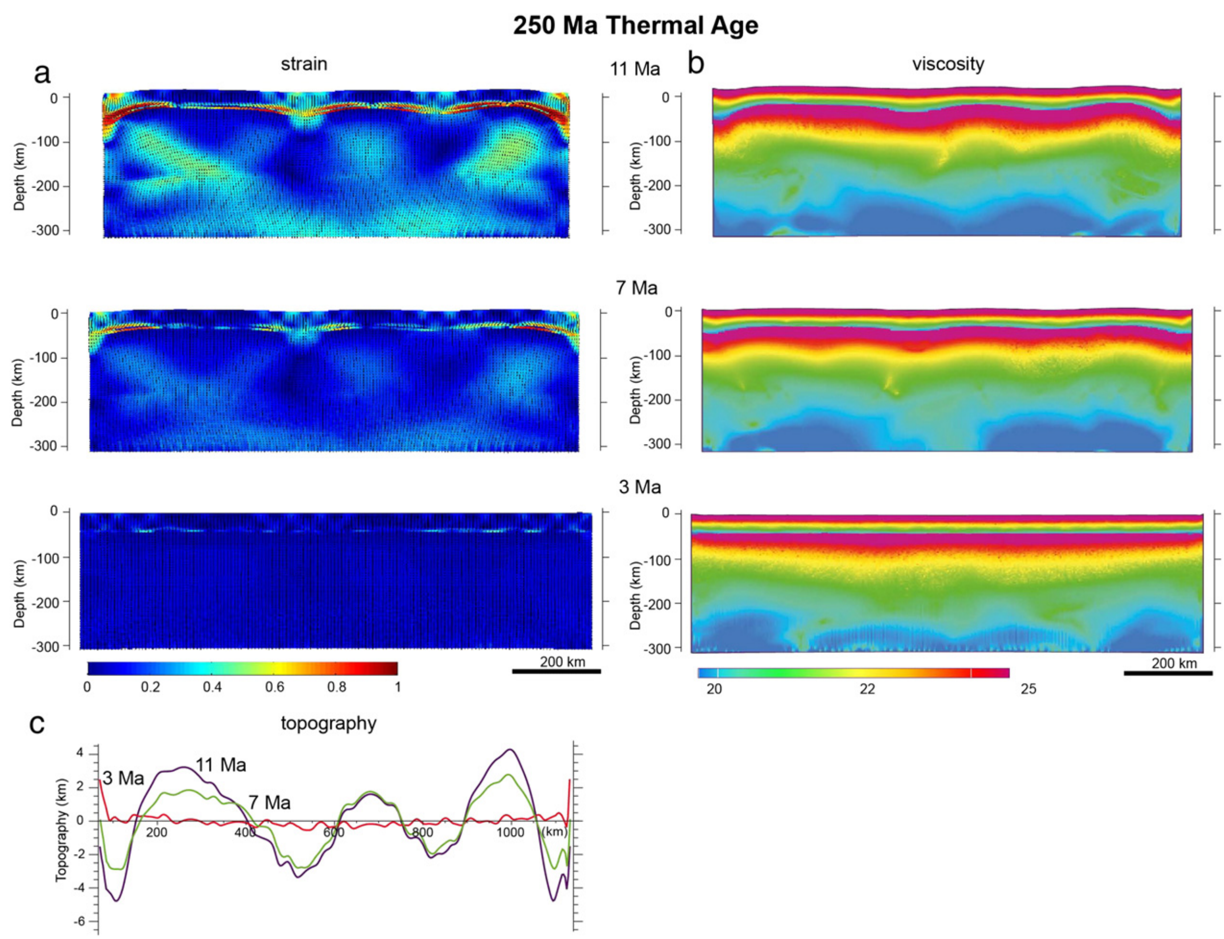

Fig. 9. Thermo-mechanical numerical model of stratified continental lithosphere showing characteristic patterns of deformation induced by folding of the continental lithosphere with time. Increasing amounts of horizontal shortening for a 250 Ma old lithosphere with a convergence rate of 1.25 cm a^{-1}. Development of short crustal wavelengths superimposed on large-scale mantle wavelengths. 250 km thick, visco-elastic–plastic continental lithosphere composed of a dry olivine mantle, 40 km thick crust with a granite upper crust and a quartz diorite lower crust. (a) strain distribution for three different time steps. b) Effective viscosity structure of the deforming lithosphere. c) Evolution of topography.

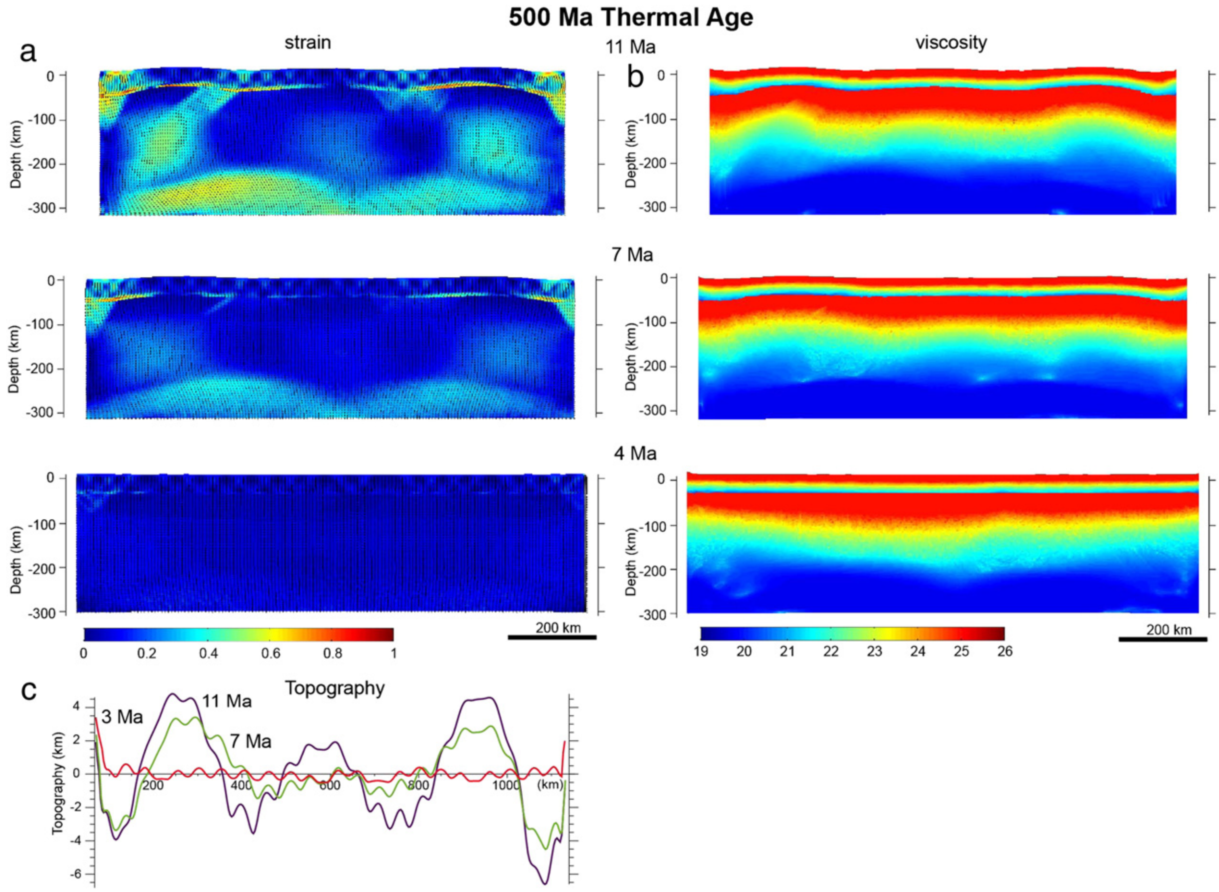

Fig. 10. Characteristic patterns of deformation induced by folding of a 500 Ma old continental lithosphere with time, the same experiment as Fig. 9 apart from the older thermo-tectonic age of the lithosphere. Increasing amounts of horizontal shortening with convergence rate of 1.25 cm a^{-1}. (a) strain distribution for three different time steps. b) Effective viscosity structure of the deforming lithosphere. c) Evolution of topography.

between intraplate deformation and basin dynamics, and the role of mantle dynamics.

6.1. Wavelengths and spatial patterns of intraplate deformation: manifestation in geophysical and crustal/lithospheric observations

As discussed previously, we have explored whether the wavelengths and spatial patterns inferred from satellite-derived topography and gravity models are consistent with lithospheric folding induced by Arabian and Indian collision with Eurasia. To this aim, wavelengths of folding have been calculated adopting rheologies and thermo-mechanical ages of the lithosphere characteristic for the area. Constraints on the magnitude of the differential topography are provided from basement deflection in the down flexed portion of the lithospheric folds and surface topography in the upward part of the folds. Both estimates are sensitive to effects of erosion and sedimentation intrinsically amplifying and reducing amplitudes respectively. In addition, constraints on amplitudes of the differential lithospheric scale geometry of the intraplate deformation are provided by gravity and seismic data and Moho deflection. As demonstrated previously and in previous work by Burov and Molnar (1998), mantle scale folding has a prime manifestation in terms of its gravity signature and Moho as well as basement topography. As shown by both analogue and numerical experiments presented here, there is a clear link in lithospheric deformation between near-surface brittle deformation and deformation at deeper levels. This applies in particular for lithospheric folding which gives rise to large wavelength deflections at deeper levels and short wavelength deformation by thrusting at or near the surface.

6.2. Interference of patterns of intraplate deformation

We have demonstrated that lithosphere scale folds can be detected in front of, and parallel to both indenters. The resulting interference generates the irregular folding illustrated by the pattern of Neogene and Quaternary outcrops. In this paper, we have explored whether the interference of lithospheric folding could explain the surface topography and gravity over this wide area in front of the Indian and Arabian indenters.

As illustrated by Fig. 13, the documented interference of the patterns of folding appears to be primarily the result of the spatial orientation of the two indenters, differences in their convergence velocities and the thermo-mechanical structure of the lithosphere west and east of the Kugitang–Tunka Line. Movement of the indenters perpendicular to the strike of these boundaries is not a pre-requisite to induce the observed trends in undulations oriented parallel to the plate boundary.

6.3. Continental collision and intraplate deformation: temporal aspects

The almost instantaneous nature of the onset of deformation rules out a thermal cause (characterised by thermal time constants of several tens of millions of years). Lithospheric instabilities such as folding, however, are associated with time constants of 0.1 to a few My, making them a feasible mechanism. Our models are also

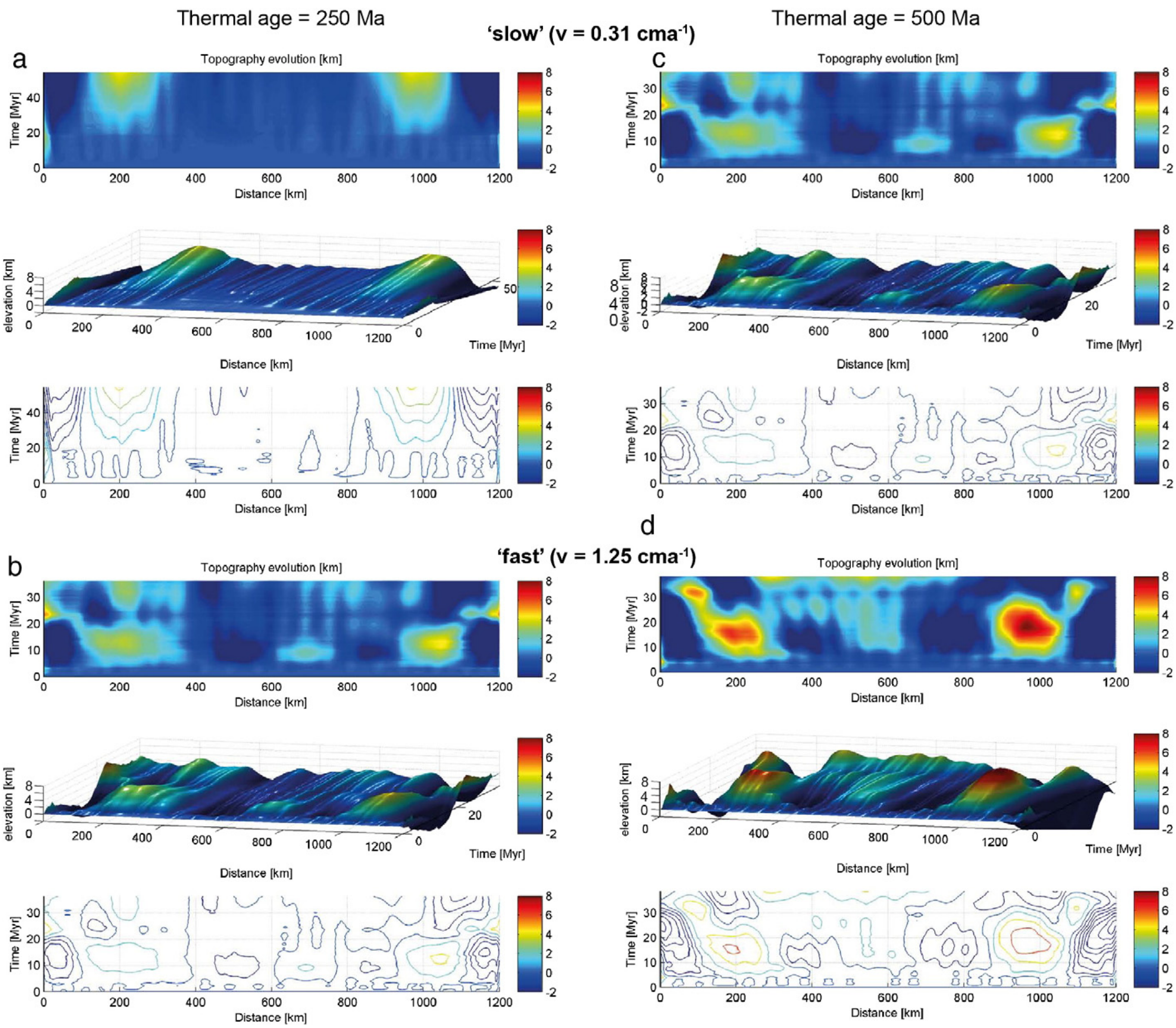

Fig. 11. Temporal evolution of topography in 2D and 3D view for slow (0.31 cm a^{-1} top) and fast (1.25 cm a^{-1}, bottom) shortening of thermo-mechanical numerical models of a stratified, 250 (left) and 500 Ma (right) old, continental lithosphere. Subpanels display topography evolution of the 2D models with time, with the bottom subpanels displaying contour lines of elevation at 2 km intervals. Note the temporal development of short crustal wavelengths superimposed on large-scale mantle wavelengths. Model setup for all four experiments corresponds to that of Fig. 9 (see also Appendix A for more detail).

consistent with outward movement of deformation, away from the orogen along the suture, such as observed from the High Zagros towards the Eurasian foreland lithosphere.

Collision is a continuous process with a number of tipping points in the associated deformation in the foreland lithosphere. In the process of continuous build-up of stresses, plate reorganisations can lead to short-term changes in orientation and magnitude of the induced stress field whereas partial stress relaxation by mechanisms such as lithosphere folding can take place in a punctuated way when stresses reach thresholds of lithospheric strength. Manifestations of short-term perturbations in stress-regime include the closure of (back)arc basins, arc accretion, mountain building by duplex formation and underthrusting along the suture followed by a shift of deformation away from the suture, inversion of basins located further away and intraplate deformation by folding.

Neogene shortening and uplift of the Alborz, Kopeh Dagh and Caucasus Mountain belts in Iran and surrounding areas is characterised by a simultaneous onset of major topography formation at ca. 5 Ma. At the same time, the adjacent Caspian, Turan and Amu Darya basins underwent accelerated subsidence.

6.4. Lithosphere folding and sedimentary basin dynamics

Obviously, a difference must be made between accommodation space and sediment supply. Sediment supply itself can never create the accommodation space needed to store 10 km of Neogene sediments for realistic estimates of palaeo-water depth. The only way to create an accommodation space of 5 km to be further amplified with a factor 2 by the density difference by water and sediments is by tectonics. In the absence of evidence for extension and in line with the overall tectonic regime and the inferred rates of differential vertical motions with uplift in the Alborz and simultaneous subsidence in the South Caspian Basin, lithosphere folding appears to be a viable mechanism. The Volga probably did not deposit the sediments further upstream, because down flexing of the South Caspian created enough accommodation space to store the enormous amounts of sediments.

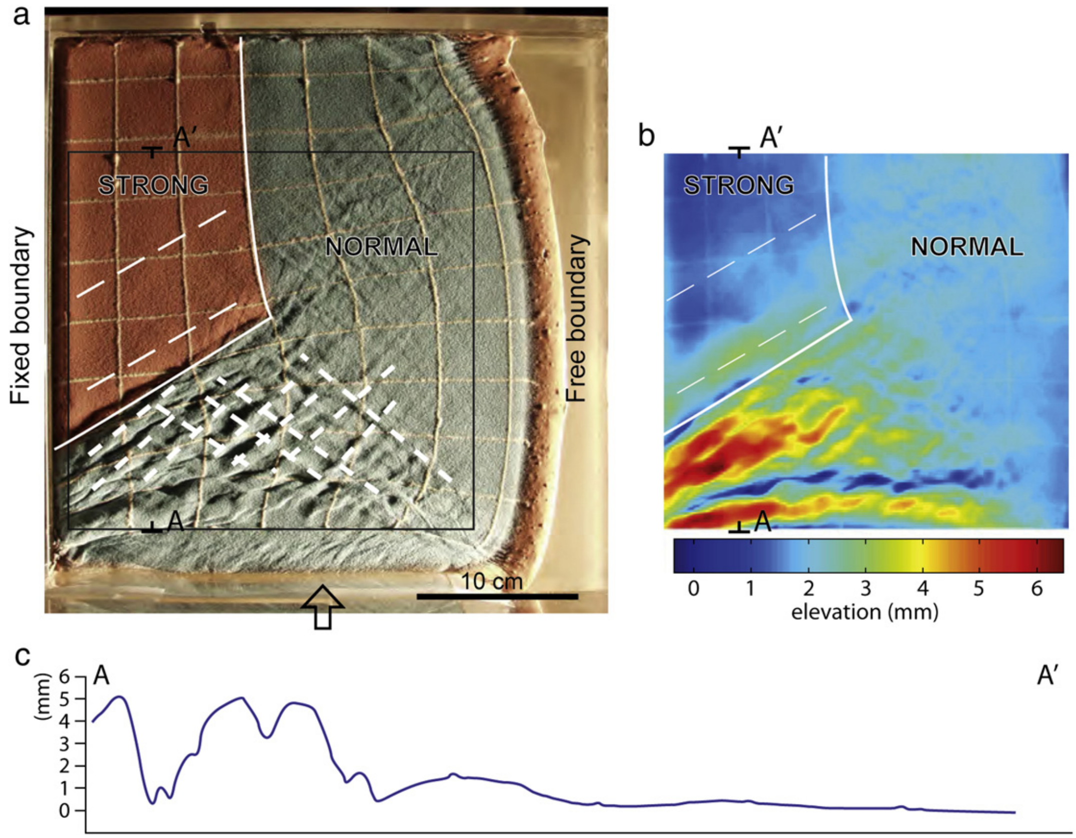

Fig. 12. a) Laboratory experiment of oblique indentation showing stress transfer across plate boundary generating plate-boundary parallel folding. a) Surface view, collision with strong lithospheric block (red, separated by white line from normal strength lithosphere (green)) induces two sets of perpendicularly trending axes of lithospheric folding in the Central Asian domain. Dashed lines in the foreland mark NW–SE oriented fold axes in the West Siberian Plate. The free boundary at right hand side diminishes the impact of folding in the upper right part of the deformed area. b) Plan view digital topography. c) Cross-section A–A′ perpendicular to the plate boundary (bottom, see location on Fig. 12b), imaged by laser scanning of surface of lithosphere deforming as a result of continental collision.

Both folding and transpression can generate mountain belts without a root such as the Alborz. Transpression could explain the case of the Turkish and Afghan orogens. Their location along the Tethyan suture in itself does not appear to play a key role.

6.5. Lithosphere folding and mantle dynamics

A mountain range, few kilometres high next to a 20 km deep basin is definitely anomalous in terms of differential topography. The substantial gravity anomalies with wavelengths of several hundreds of kilometres are characteristic for lithosphere scale deformation including an upper mantle component. It is exactly for this reason that various authors have emphasised the need for a contribution by lithosphere dynamics such as incipient subduction (e.g., Jackson et al., 2002). Others have presented evidence for recent slab break-off under the southeastern Zagros Mountains (e.g., Hafkenscheid et al., 2006; Molinaro et al., 2005) and beneath eastern Turkey and the Caucasus (Zor, 2008). As pointed out by Cloetingh et al. (2004), slab break-off will have important consequences on the regional stress field enhancing compressional deformation, eventually leading to folding in the overriding plate, whereas lithospheric folding itself can be the precursor for incipient subduction (Burov and Cloetingh, 2009, 2010). In this context, evidence for incipient subduction under the northern rim of the South Caspian Basin (Jackson et al., 2002) is particularly interesting. The models presented here show that the presence of a suture zone separating different lithospheric blocks strongly amplifies the deflection of the lithosphere leading to a deep synclinal depression flanked by more modest and narrower anticlines (Guest et al., 2007; Sokoutis et al., 2005). Our results also shed light on findings from recent studies of other segments of the Alpine–Himalayan collision zone, such as Iberia and northern Africa. Numerical modelling studies of the Cenozoic intraplate deformation of Iberia have demonstrated the important role of lithospheric heterogeneities in the location of intraplate deformation (Martín-Velázquez and De Vicente, 2012). Babault et al. (2008) and Ghorbal et al. (2008) have presented evidence for late Cenozoic vertical motions in stable parts of NW-Africa with long-wavelength surface uplift patterns typical for lithospheric folding. The documented kilometre-scale differential topography with rapid subsidence of the Moroccan Atlantic margin and elevated young topography in the Atlas Mountains and adjacent areas of the NW African continent such as the Algerian Mediterranean margin, interpreted as sites of incipient subduction (Baes et al., 2011; Déverchère et al., 2005) are all occurring in a regime of present-day compression.

7. Conclusions

The intraplate deformation in western Central Asia is characterised by spatial and temporal patterns pointing to lithospheric folding as a major mode for generating the observed patterns in differential topography, lithosphere geometry and basin dynamics. The wavelengths of the observed lithosphere deformation are consistent with the inferences from thermo-mechanical models constructed for the lithosphere in western Central Asia. Analogue and numerical models of intraplate deformation induced by two simultaneously acting indenters, provide a self-consistent explanation for the observed interference of spatial patterns of lithosphere deformation in western Central Asia. Differences

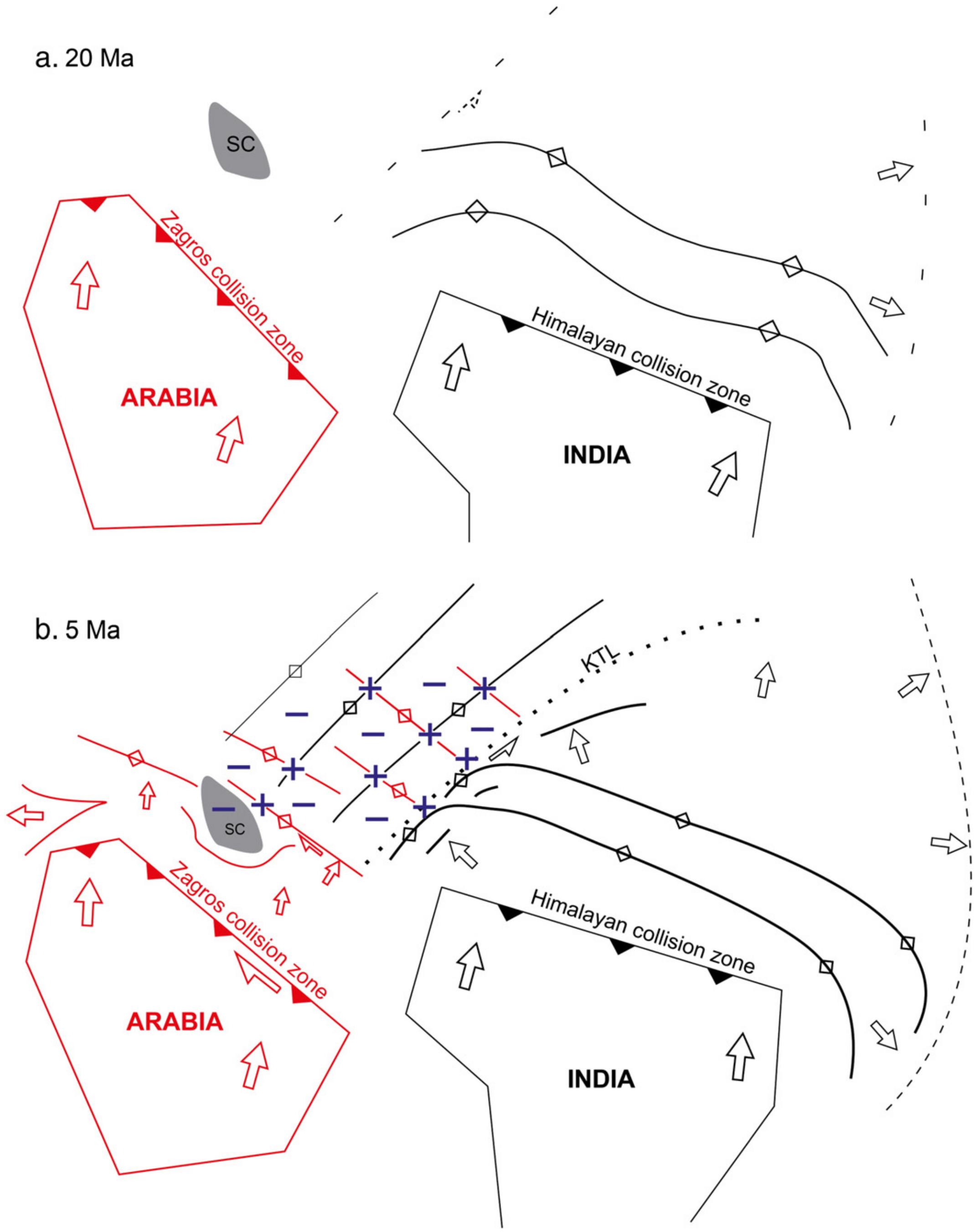

Fig. 13. Cartoon summarising the connection between temporal evolution in convergence history of India, Arabia and Eurasia and spatial patterns of large-scale intraplate deformation in Central Asia. Interference of folding axes (indicated by solid lines with diamond) leads to enhanced differential vertical motions (+: uplift, −: subsidence). SC: South Caspian; KTL: Kugitang–Tunka Line. Arrows mark directions of horizontal motion. a) 20 Ma, corresponding to ongoing collision along the Himalayan front and folding in its foreland and early phase of collision along the Zagros. b) 5 Ma, corresponding to enhanced plate coupling in the Zagros and related northward propagation of deformation, creating folding in and around the Turan platform, interacting with folding induced by westward directed stress field parallel to the Kugitang–Tunka Line.

in the convergence velocities of the Indian and Arabian indenters with respect to Eurasia and spatial variations in thermo-mechanical structure of the lithosphere west and east of the Kugitang–Tunka Line appear to of key importance.

Acknowledgements

Constructive reviews by D. van Hinsbergen and S. Schmalholz are acknowledged. Funding was provided by SNF, The Netherlands Research Centre for Integrated Solid Earth Sciences and ISTeP, UPMC. SC acknowledges ETH and UPMC for visiting professorships.

Appendix A. Supplementary data

Supplementary data to this article can be found online at http://dx.doi.org/10.1016/j.tecto.2012.10.032.

References

Agard, P., Omrani, J., Jolivet, L., Whitechurch, H., Vrielynck, B., Spakman, W., Monié, P., Meyer, B., Wortel, R., 2011. Zagros orogeny: a subduction-dominated process. Geological Magazine 148, 692–725.

Avdeev, B., Niemi, N.A., 2011. Rapid Pliocene exhumation of the central Greater Caucasus constrained by low-temperature thermochronometry. Tectonics 30, TC2009. http://dx.doi.org/10.1029/2010TC002808.
Avouac, J.P., Burov, E.B., 1996. Erosion as a driving mechanism of intracontinental mountain growth. Journal of Geophysical Research 101, 17747–17769. http://dx.doi.org/10.1029/96jb01344.
Axen, G.J., Lam, P.J., Grove, M., Stockli, D.F., Hassanzadeh, J., 2001. Exhumation of the west-central Alborz Mountains, Iran, Caspian subsidence, and collision-related tectonics. Geology 29, 559–562.
Babault, J., Teixelll, A., Arboleya, M.L., Charroud, M., 2008. A Late Cenozoic age for long-wavelength surface uplift of the Atlas Mountains of Morocco. Terra Nova 20, 102–107.
Baes, Ma, Govers, R., Wortel, R., 2011. Subduction initiation along the inherited weakness zone at the edge of a slab: insights from numerical models. Geophysical Journal International 184. http://dx.doi.org/10.1111/j.1365-246X.2010.04896.x.
Belousov, T.P., Mukhamediev, S.A., Kurtasov, S.F., 2001. Joint orientations from Paleozoic sedimentary rocks in the Kyzyl Kum region, Uzbekistan. Central Asia. Russ. J. Earth Sci. 3, 333–351.
Bird, P., 1991. Lateral extrusion of lower crust from under high topography in the isostatic limit. Journal of Geophysical Research 96, 10275–10286.
Bonini, M., Corti, G., Sokoutis, D., Vannucci, G., Gasperini, P., Cloetingh, S., 2003. Insights from scaled analogue modelling into the seismotectonics of the Iranian region. Tectonophysics 376, 137–1493.
Bourgeois, O., Ford, M., Diraison, M., Carlier, Le, de Veslud, C., Gerbault, M., Pik, R., Nuby, N., Bonnet, S., 2007. Separation of rifting and lithospheric folding signatures in the NW-Alpine foreland. International Journal of Earth Sciences 96, 1003–1031.
Brunet, M.-F., Cloetingh, S. (Eds.), 2003. Integrated Peri-Tethyan Basins studies (Peri-Tethys Programme). Sedimentary Geology, vol. 156, p. 288.
Brunet, M.-F., Granath, J.W., Wilmsen, M., 2009. South Caspian to Central Iran basins: introduction. Geological Society of London, Special Publication 312, 1–6.
Burg, J.P., Podladchikov, Y., 1999. Lithospheric scale folding; numerical modelling and application to the Himalayan syntaxes. International Journal of Earth Sciences 88, 190–200.
Burg, J.P., Podladchikov, Y., 2000. From buckling to asymmetric folding of the continental lithosphere: numerical modelling and application to the Himalayan syntaxes. Geological Society of London, Special Publication 170, 219–236. http://dx.doi.org/10.1144/GSL.SP.2000.170.01.12.
Burg, J.P., Schmalholz, S.M., 2008. Viscous heating allows thrusting to overcome crustal-scale buckling: numerical investigation with application to the Himalayan syntaxes. Earth and Planetary Science Letters 274, 189–203.
Burg, J.P., Davy, P., Martinod, J., 1994. Shortening of analogue models of the continental lithosphere; new hypothesis for the formation of the Tibetan Plateau. Tectonics 13, 475–483.
Burov, E., Cloetingh, S., 2009. Controls of mantle plumes and lithospheric folding on modes of intra-plate continental tectonics: differences and similarities. Geophysical Journal International 178, 1691–1722.
Burov, E., Cloetingh, S., 2010. Plume-like upper mantle instabilities drive subduction initiation. Geophysical Research Letters 37, L03309.
Burov, E.B., Molnar, P., 1998. Gravity anomalies over the Ferghana Valley (Central Asia) and intracontinental deformation. Journal of Geophysical Research 103, 18,137–18,152.
Burov, E.V., Kogan, M.G., Lyon-Caen, H., Molnar, P., 1990. Gravity anomalies, the deep structure, and dynamic processes beneath the Tien Shan. Earth and Planetary Science Letters 96, 367–383.
Burov, E.B., Lobkovsky, L.I., Cloetingh, S., Nikishin, A.M., 1993. Continental lithosphere folding in Central Asia (part II): constraints from gravity and topography. Tectonophysics 226, 73–87.
Burov, E., Jaupart, C., Mareschal, J.C., 1998. Large-scale crustal heterogeneities and lithospheric strength in cratons. Earth and Planetary Science Letters 164, 205–219.
Buslov, M.M., De Grave, J., Bataleva, E.A.V., Batalev, V.Y., 2007. Cenozoic tectonic and geodynamic evolution of the Kyrgyz Tien Shan Mountains: a review of geological, thermochronological and geophysical data. Journal of Asian Earth Sciences 29, 205–214.
Buslov, M.M., Kokh, D.A., De Grave, J., 2008. Mesozoic–Cenozoic tectonics and geodynamics of Altai, Tien Shan, and Northern Kazakhstan, from apatite fission-track data. Russian Geology and Geophysics 49, 648–654.
Calais, E., Dong, L., Wang, M., Shen, Z., Vergnolle, M., 2006. Continental deformation in Asia from a combined GPS solution. Geophysical Research Letters 33, L24319.
Charreau, J., Chen, Y., Gilder, S., Barrier, L., Dominguez, S., Augier, R., Sen, S., Avouac, J.-P., Gallaud, A., Graveleau, F., Wang, Q., 2009. Neogene uplift of the Tian Shan Mountains observed in the magnetic record of the Jingou River section (northwest China). Tectonics 28, TC2008. http://dx.doi.org/10.1029/2007tc002137.
Cloetingh, S., Burov, E., 2011. Lithospheric folding and sedimentary basin evolution: a review and analysis of formation mechanisms. Basin Research 23, 257–290. http://dx.doi.org/10.1111/j.1365-2117.2010.00490.x.
Cloetingh, S., Burov, E., Poliakov, A., 1999. Lithosphere folding; primary response to compression? (from Central Asia to Paris Basin). Tectonics 18, 1064–1083.
Cloetingh, S.A.P.L., Burov, E., Matenco, L., Toussaint, G., Bertotti, G., Andriessen, P.A.M., Wortel, M.J.R., Spakman, W., 2004. Thermo-mechanical controls on the mode of continental collision in the SE Carpathians (Romania). Earth and Planetary Science Letters 218, 57–76. http://dx.doi.org/10.1016/S0012-821X(03)00645-9.
Cloetingh, S., Beekman, F., Ziegler, P.A., van Wees, J.-D., Sokoutis, D., 2008. Post-rift compressional reactivation potential of passive margins and extensional basins. Geological Society of London, Special Publication 306, 27–70.
Cloetingh, S., et al., 2010. Lithosphere tectonics and thermo-mechanical properties: an integrated modelling approach for Enhanced Geothermal Systems exploration in Europe. Earth-Science Reviews 102, 159–206.
Cobbold, P.R., Davy, P., Gapais, D., Rossello, E.A., Sadybakasov, E., Thomas, J.C., Tondji Biyo, J.J., de Urreiztieta, M., 1993. Sedimentary basins and crustal thickening. Sedimentary Geology 86, 77–89.
Cunningham, D., 2005. Active intracontinental transpressional mountain building in the Mongolian Altai: defining a new class of orogen. Earth and Planetary Science Letters 240, 436–444.
Davy, P., Cobbold, P.R., 1991. Experiments on shortening of a 4-layer model of the continental lithosphere. Tectonophysics 188, 1–25.
De Grave, J., Buslov, M.M., Van den haute, P., 2007. Distant effects of India–Eurasia convergence and Mesozoic intracontinental deformation in Central Asia: constraints from apatite fission-track thermochronology. Journal of Asian Earth Sciences 29, 188–204.
Déverchère, J., Yelles, K., Domzig, A., Mercier De Lepinay, B., Bouillin, J.P., Gaullier, V., Bracene, R., Calais, E., Savoye, B., Kherroubi, A., Le Roy, P., Pauc, H., Dan, G., 2005. Active thrust faulting offshore Boumerdes, Algeria, and its relations to the 2003 Mw 6.9 earthquake. Geophysical Research Letters 32, L043111.
Devlin, W.J., Cogswellll, J.M., Gaskins, G.M., Isaksen, G.H., Pitcher, D.M., Pius, D.P., Stanley, K.O., Wall, J.R.T., 1999. South Caspian Basin: young, cool, and full of promise. GSA Today 9, 1–9.
Dewey, J.F., Hempton, M.R., Kidd, W.S.F., Saroglu, F., Sengor, A.M.C., 1986. Shortening of continental lithosphere: the neotectonics of Eastern Anatolia — a young collision zone. Geological Society of London, Special Publication 19, 1–36. http://dx.doi.org/10.1144/gsl.sp.1986.019.01.01.
Dombrádi, E., Sokoutis, D., Bada, G., Cloetingh, S., Horváth, F., 2010. Modelling recent deformation of the Pannonian lithosphere: lithospheric folding and tectonic topography. Tectonophysics 484, 103–118.
Egan, S.S., Mosar, J., Brunet, M.-F., Kangarli, T., 2009. Subsidence and uplift mechanisms within the South Caspian Basin: insights from the onshore and offshore Azerbaijan region. Geological Society of London, Special Publication 312, 219–240.
Fernández-Lozano, J., Sokoutis, D., Willingshofer, E., Cloetingh, S., De Vicente, G., 2011. Cenozoic deformation of Iberia: a model for intraplate mountain building and basin development based on analogue modeling. Tectonics 30, TC1001. http://dx.doi.org/10.1029/2010tc002719.
Forte, A.M., Cowgill, E., Bernardin, T., Kreylos, O., Hamann, B., 2010. Late Cenozoic deformation of the Kura fold–thrust belt, southern Greater Caucasus. Geological Society of America Bulletin 122, 465–486.
Fu, B., Ninomiya, Y., Guo, J., 2010. Slip partitioning in the northeast Pamir–Tian Shan convergence zone. Tectonophysics 483, 344–364.
Garcia-Castellanos, D., Cloetingh, S., 2011. Modeling the interaction between lithospheric and surface processes in foreland basins. In: Busby, C., Azor, A. (Eds.), Recent Advances in Tectonics of Sedimentary Basins. Wiley-Blackwell, pp. 152–184.
Garzanti, E., Gaetani, M., 2002. Unroofing history of Late Paleozoic magmatic arcs within the "Turan Plate" (Tuarkyr, Turkmenistan). Sedimentary Geology 151, 67–87.
Geller, C.A., Weissel, J.K., Anderson, R.N., 1983. Heat transfer and intraplate deformation in the central Indian Ocean. Journal of Geophysical Research 88, 1018–1032.
Gerbault, M., Burov, E., Poliakov, A., Dagnieres, M., 1999. Do faults trigger folding in the lithosphere? Geophysical Research Letters 26, 271–274.
Ghorbal, B., Bertotti, G., Foeken, J., Andriessen, P., 2008. Unexpected Jurassic to Neogene vertical movements in "stable" parts of NW Africa revealed by low temperature geochronology. Terra Nova 20, 363–553.
Ghosh, S.K., Ramberg, H., 1968. Buckling experiments on intersecting fold patterns. Tectonophysics 5, 89–105.
Ghosh, S.K., Khan, D., Sengupta, S., 1995. Interfering folds in constrictional deformation. Journal of Structural Geology 17, 1361–1373.
Grujić, D., 1993. The influence of initial fold geometry on type 1 and type 2 interference patterns: an experimental approach. Journal of Structural Geology 15, 293–307.
Guest, B., Stockli, D.F., Grove, M., Axen, G.J., Lam, P.S., Hassanzadeh, J., 2006. Thermal histories from the central Alborz Mountains, northern Iran: implications for the spatial and temporal distribution of deformation in northern Iran. Geological Society of America Bulletin 118, 1507–1521.
Guest, B., Guest, A., Axen, G., 2007. Late Tertiary tectonic evolution of northern Iran: a case for simple crustal folding. Global and Planetary Change 58, 435–453.
Hafkenscheid, E., Wortel, M.J.R., Spakman, W.J., 2006. Subduction history of the Tethyan region derived from seismic tomography and tectonic reconstructions. Geophysical Research 111, B08401. http://dx.doi.org/10.1029/2005JB003791.
Hatzfeld, D., Molnar, P., 2010. Comparisons of the kinematics and deep structures of the Zagros and Himalaya and of the Iranian and Tibetan Plateaus and geodynamic implications. Reviews of Geophysics 48, RG2005.
Heermance, R.V., Chen, J., Burbank, D.W., Miao, J., 2008. Temporal constraints and pulsed Late Cenozoic deformation during the structural disruption of the active Kashi foreland, northwest China. Tectonics 27, TC6012.
Holford, S., Green, P., Duddy, I., Turner, J., Hillis, R., Stoker, M., 2009. Regional intraplate exhumation episodes related to plate-boundary deformation. Geological Society of America Bulletin 121, 1611.
Hüsing, S.K., Zachariasse, W.-J., van Hinsbergen, D.J.J., Krijgsman, W., Inceöz, M., Harzhauser, M., Mandic, O., Kroh, A., 2009. Oligocene–Miocene basin evolution in SE Anatolia, Turkey: constraints on the closure of the eastern Tethys gateway. Geological Society of London, Special Publication 311, 107–132.
Jaboyedoff, M., Derron, M.-H., Manby, G.M., 2005. Note on seismic hazard assessment using gradient of uplift velocities in the Turan block (Central Asia). Natural Hazards and Earth System Sciences 5, 43–47.
Jackson, J., Priestley, K., Allen, M., Berberian, M., 2002. Active tectonics of the South Caspian Basin. Geophysical Journal International 148, 214–245.
Johnson, H., Doré, A., Gatliff, R., Holdsworth, R., Lundin, E., Ritchie, J. (Eds.), 2008. The nature and origin of compression in passive margins. Geol. Soc. Spec. Publ., London (306 pp.).

Kaban, M.K., 2002. A gravity model of the north Eurasia crust and upper mantle: 2. The Alpine–Mediterranean foldbelt and adjacent structures of the southern former USSR. Russian Journal of Earth Sciences 4, 19–33.
Kadinsky-Cade, K., Barazangi, M., Oliver, J., Isacks, B., 1981. Lateral variations of high-frequency seismic wave propagation at regional distances across the Turkish and Iranian Plateaus. Journal of Geophysical Research 86, 9377–9396.
Kaus, B.J.P., Schmalholz, S.M., 2006. 3D finite amplitude folding: implications for stress evolution during crustal and lithospheric deformation. Geophysical Research Letters 33, L14309.
Kogan, M., McNutt, M., 1987. Isostasy in the USSR I: admittance data, composition, structure and dynamics of the lithosphere–asthenosphere system, 3 ed. In: Fuchs, K., Froidevaux, C. (Eds.), Geodynamics Ser., 16. Amer. Geophys. Union, pp. 301–307.
Le Dortz, K., Meyer, B., Sébrier, M., Braucher, R., Nazari, H., Benedetti, L., Fattahim, M., Bourlès, D., Foroutan, M., Siame, L., Rashidi, A., Bateman, M.D., 2011. Dating inset terraces and offset fans along the Dehshir Fault (Iran) combining cosmogenic and OSL methods. Geophysical Journal International 1147–1174. http://dx.doi.org/10.1111/j.1365-246X.2011.05010.x.
Lechmann, S.M., May, D.A., Kaus, B.J.P., Schmalholz, S.M., 2011. Comparing thin-sheet models with 3D multilayer models for continental collision. Geophysical Journal International 187, 10–33.
Liu, Z., Bird, P., 2008. Kinematic modelling of neotectonics in the Persia–Tibet–Burma orogen. Geophysical Journal International 172, 779–797.
Liu, M., Mooney, W.D., Li, S., Okaya, N., Detweiler, S., 2006. Crustal structure of the northeast margin of the Tibetan Plateau from the Songpan–Ganzi terrane to the Ordos Basin. Tectonophysics 420, 253–266.
Lyberis, N., Manby, G., 1999. Oblique to orthogonal convergence across the Turan Block in the post-Miocene. AAPG Bulletin 83, 1135–1160.
Mangino, S., Priestley, K., 1998. The crustal structure of the southern Caspian region. Geophysical Journal International 133, 630–648.
Martinod, J., Davy, P., 1994. Periodic instabilities during compression of the lithosphere; 2. Analogue experiments. Journal of Geophysical Research 99, 12,057–12,069.
Martín-Velázquez, S., de Vicente, G., 2012. The role of lithospheric heterogeneities in the location of the Cenozoic intraplate deformation of Iberia from finite element modeling. Tectonics 31, TC1009. http://dx.doi.org/10.1029/2011tc002954.
McAdoo, D.C., Sandwell, D.T., 1985. Folding of oceanic lithosphere. Journal of Geophysical Research 90, 8563–8569.
Mohadjer, S., Bendick, R., Ischuk, A., Kuzikov, S., Kostuk, A., Saydullaev, U., Lodi, S., Kakar, D.M., Wasy, A., Khan, M.A., Molnar, P., Bilham, R., Zubovich, A.V., 2010. Partitioning of India–Eurasia convergence in the Pamir–Hindu Kush from GPS measurements. Geophysical Research Letters 37, L04305. http://dx.doi.org/10.1029/2009gl041737.
Molinaro, M., Zeyen, H., Laurencin, X., 2005. Lithospheric structure beneath the south-eastern Zagros Mountains, Iran: recent slab break-off? Terra Nova 17, 1–6.
Molnar, P., Tapponnier, P., 1975. Cenozoic tectonics of Asia: effects of a continental collision. Science 189, 419–426.
Mouthereau, F., Lacombe, O., Vergés, J., 2012. Building the Zagros collisional orogen: timing, strain distribution and the dynamics of Arabia/Eurasia plate convergence. Tectonophysics 532–535, 27–60.
Muñoz-Martín, A., De Vicente, G., Fernández-Lozano, J., Cloetingh, S., Willingshofer, E., Sokoutis, D., Beekman, F., 2010. Spectral analysis of the gravity and elevation along the western Africa–Eurasia plate tectonic limit: continental versus oceanic lithospheric folding signals. Tectonophysics 495, 298–314.
Munteanu, I., Matenco, L., Dinu, C., Cloetingh, S., 2011. Kinematics of back-arc inversion of the western Black Sea Basin. Tectonics 30, TC5004.
Nadirov, R.S., Bagirov, E., Tagiyev, M., Lerche, I., 1997. Flexural plate subsidence, sedimentation rates and structural development of the super-deep south Caspian Basin. Marine and Petroleum Geology 14, 383–400.
Nikishin, A.M., Cloetingh, S., Lobkovsky, L.I., Burov, E.B., Lankreijer, A.C., 1993. Continental lithosphere folding in Central Asia; Part I. Constraints from geological observations. Tectonophysics 226, 59–72.
Nikishin, A.M., Brunet, M.F., Cloetingh, S., Ershov, A.V., 1997. Northern Peri-Tethyan Cenozoic intraplate deformations: influence of the Tethyan collision belt on the Eurasian continent from Paris to Tian-Shan. Comptes Rendus de l'Académie Bulgare des Sciences 324, 49–57.
Nikishin, A.M., Ziegler, P.A., Abbott, D., Brunet, M.F., Cloetingh, S., 2002. Permo-Triassic intraplate magmatism and rifting in Eurasia: implications for mantle plumes and mantle dynamics. Tectonophysics 351, 3–39.
Ramsay, J.G., 1967. Folding and Fracturing of Rocks. McGraw-Hill, New York.
Regard, V., Hatzfeld, D., Molinaro, M., Aubourg, C., Bayer, R., Bellier, O., Yamini-Fard, F., Peyret, M., Abbassi, M., 2004. The transition between Makran subduction and the Zagros collision: recent advances in its structure and active deformation. Geological Society of London, Special Publication 330, 43–64. http://dx.doi.org/10.1144/SP330.4.
Reilinger, R., McClusky, S., 2011. Nubia–Arabia–Eurasia plate motions and the dynamics of Mediterranean and Middle East tectonics. Geophysical Journal International 186, 971–979.
Reiter, K., Kukowski, N., Ratschbacher, L., 2011. The interaction of two indenters in analogue experiments and implications for curved fold-and-thrust belts. Earth and Planetary Science Letters 302, 132–146. http://dx.doi.org/10.1016/j.epsl.2010.12.002.
Ryan, W.B.F., et al., 2009. Global multi-resolution topography synthesis. Geochemistry, Geophysics, Geosystems 10, Q03014. http://dx.doi.org/10.1029/2008GC002332.
Schmalholz, S.M., 2008. 3D numerical modeling of forward folding and reverse unfolding of a viscous single-layer: implications for the formation of folds and fold patterns. Tectonophysics 446, 31–41.
Schmalholz, S.M., Kaus, B.J.P., Burg, J.-P., 2009. Stress–strength relationship in the lithosphere during continental collision. Geology 37, 775–778.
Schmid, D.W., Dabrowski, M., Krotkiewski, M., 2008. Evolution of large amplitude 3D fold patterns: a FEM study. Physics of the Earth and Planetary Interiors 171, 400–408.
Sengör, A.M.C., Görür, N., Saroglu, F., 1985. Strike–slip faulting and related basin formation in zones of tectonic escape; Turkey as a case study. Strike–slip deformation, basin formation, and sedimentation: In: Biddle, K.T., Christie-Blick, N. (Eds.), Soc. Econ. Paleont. Miner. publ., 37, pp. 227–264 (Tulsa, OK).
Shin, Y.H., Shum, C.-K., Braitenberg, C., Lee, S.M., Xu, H., Choi, K.S., Baek, J.H., Park, J.U., 2009. Three-dimensional fold structure of the Tibetan Moho from GRACE gravity data. Geophysical Research Letters 36, L01302.
Simón, J.L., 2004. Superposed buckle folding in the eastern Iberian Chain, Spain. Journal of Structural Geology 26, 1447–1464.
Smit, J., Brun, J.P., Cloetingh, S., Ben-Avraham, Z., 2010. The rift-like structure and asymmetry of the Dead Sea Fault. Earth and Planetary Science Letters 290, 74–82. http://dx.doi.org/10.1016/j.epsl.2009.11.060.
Sobel, E.R., Chen, J., Heermance, R.V., 2006. Late Oligocene–Early Miocene initiation of shortening in the southwestern Chinese Tian Shan: implications for Neogene shortening rate variations. Earth and Planetary Science Letters 247, 70–81. http://dx.doi.org/10.1016/j.epsl.2006.03.048.
Sobel, E.R., Schoenbohm, L.M., Chen, J., Thiede, R., Stockli, D.F., Sudo, M., Strecker, M.R., 2011. Late Miocene–Pliocene deceleration of dextral slip between Pamir and Tarim: implications for Pamir orogenesis. Earth and Planetary Science Letters 304, 369–378.
Sodoudi, F., Yuan, X., Kind, R., Heit, B., Sadidkhouy, A., 2009. Evidence for a missing crustal root and a thin lithosphere beneath the Central Alborz by receiver function studies. Geophysical Journal International 177, 733–742.
Sokoutis, D., Burg, J.-P., Bonini, M., Corti, G., Cloetingh, S., 2005. Lithospheric-scale structures from the perspective of analogue continental collision. Tectonophysics 406, 1–15.
Stein, C.A., Cloetingh, S., Wortel, R., 1989. Seasat derived gravity constraints on stress and deformation in the northeastern Indian Ocean. Geophysical Research Letters 16, 823–826.
Stephenson, R.A., Lambeck, K., 1985. Isostatic response of the lithosphere with in-plane stress: application to Central Australia. Journal of Geophysical Research 90, 8581–8588.
Tesauro, M., Kaban, M., Cloetingh, S., 2012. Global strength and elastic thickness of the lithosphere. Global and Planetary Change 90–91, 51–57. http://dx.doi.org/10.1016/j.gloplacha.2011.12.003.
Tesauro, M., Kaban, M.K., Cloetingh, S.A.P.L., 2013. Global model for the lithospheric strength and effective elastic thickness. Tectonophysics 602, 78–86 (this issue).
Thomas, J.-C., Grasso, J.-R., Bossu, R., Martinod, J., Nurtaev, B., 1999a. Recent deformation in the Turan and South Kazakh platforms, western central Asia, and its relation to Arabia–Asia and India–Asia collisions. Tectonics 18, 201–214.
Thomas, J.C., Cobbold, P.R., Shein, V.S., Le Douaran, S., 1999b. Sedimentary record of late Paleozoic to Recent tectonism in central Asia: analysis of subsurface data from the Turan and south Kazak domains. Tectonophysics 313, 243–263.
van der Pluijm, B.A., Craddock, J.P., Graham, B.R., Harris, J.H., 1997. Paleostress in Cratonic North America: implications for deformation of continental interiors. Science 277, 794–796.
van Hinsbergen, D.J.J., Kapp, P., Dupont-Nivet, G., Lippert, P.C., DeCelles, P.G., Torsvik, T.H., 2011. Restoration of Cenozoic deformation in Asia and the size of Greater India. Tectonics 30, TC5003.
Vergnolle, M., Calais, E., Dong, L., 2007. Dynamics of continental deformation in Asia. Journal of Geophysical Research 112, B11403.
Yin, A., 2010. Cenozoic tectonic evolution of Asia: a preliminary synthesis. Tectonophysics 488, 293–325. http://dx.doi.org/10.1016/j.tecto.2009.06.002.
Ziegler, P.A., Cloetingh, S., van Wees, J.-D., 1995. Dynamics of intraplate compressional deformation: the Alpine foreland and other examples. Tectonophysics 252, 7–59.
Ziegler, P.A., van Wees, J.-D., Cloetingh, S.A.P.L., 1998. Mechanical controls on collision-related compressional intraplate deformation. Tectonophysics 300, 103–129.
Zor, E., 2008. Tomographic evidence of slab detachment beneath eastern Turkey and the Caucasus. Geophysical Journal International 175, 1273–1282.
Zubovich, A.V., et al., 2010. GPS velocity field for the Tien Shan and surrounding regions. Tectonics 29, TC6014.